

ELECTRICAL COMMUNICATION

*Technical Journal of the
International Telephone and Telegraph Corporation
and Associate Companies*

SOUND REINFORCEMENT AND PRODUCTION FOR ROYAL FESTIVAL HALL

AUTOMATIC SELECTIVE TUBE SYSTEM AT BRIDGEPORT BRASS COMPANY

TECHNIQUE OF TRUSTWORTHY VALVES

APPLICATION OF 12-CHANNEL CARRIER TO BRAZILIAN OPEN-WIRE LINE

PIEZOELECTRIC CONSTANTS OF SOME ISOMORPHOUS CRYSTALS

GAS DISCHARGE PLASMA IN HIGH-FREQUENCY ELECTROMAGNETIC FIELDS

MAGNETO-OPTICS OF AN ELECTRON GAS IN RECTANGULAR WAVEGUIDE



Volume 28

DECEMBER, 1951

Number 4

The results of the surveys were examined in detail and it was found possible, by moving just under 200 poles (excluding those that had to be substituted), to reduce the sum of the squares of the transposition pole-spacing deviations (feet squared) for the repeater sections Cachoeira Paulista to Caçapava and Caçapava to Tatuapé from about 2.85 and 3.45 times the repeater section lengths (feet) to about 1.07 and 1.35, respectively.

Later, the figure for the section between Caçapava and Tatuapé was further reduced to about 1.20 by the installation of a span-type transposition arrangement described in Section 5.6 on the four *SOJ* pairs in two places where a river and a gully, respectively, prevented the location of poles.

Details of the arrangement of the transposition sections are given in Table 4 for the section from Cachoeira Paulista to Caçapava. From this table, it will be seen that there are five *J-5AA* sections coordinated with alternate-arm long-*A* sections and one *J-5D* coordinated with an alternate-arm *2R* section, the remainder of the sections, except the first three, being applied on an uncoordinated basis. The first section, a *J-5F*, runs on a spur line of four spans from the terminal pole in Cachoeira Paulista to the existing line, which it joins near the *X* transposition point of the alternate-arm long-*A* section (13/16 of the section), and thence runs for four spans on the existing line. The *J-5E* and *J-5D* sections, which follow it, are not applied on an uncoordinated basis with the remainder of the alternate-arm section, since their average transposition intervals are almost exactly half that of the long-*A* section.

It will be seen also that all transposition sections are within their design lengths except for four *J-5AA* sections (which are all less than 1.5 percent too long) and three shorter sections, which are between 3.5 and 8 percent too long. Table 4 also emphasizes the difficulty that would be experienced if septuple extra transposition points were to be established on the *J-5AA* sections in the event of applying the second-arm transposition arrangement.

For the section from Caçapava to Tatuapé, there are nine *J-5AA* sections coordinated with alternate-arm long-*A* sections, one *J-5B* coordinated with a short-*L*, and one *J-5C* coordi-

nated with a short-*L*. A *J-5C* and a *J-5D* are applied with a short-*L* on an uncoordinated basis. All the *J-5AA* sections are longer than their designed length, the worst being 1.65 percent too long, and all the short sections are within their design lengths. The difficulty in applying the *J-5* second-arm arrangement would be even greater for this repeater section than for the other, since the sum of the squares of the pole-spacing deviations would be about 5.3 times the length of the section.

On each repeater section, there were a few cases where spans greater than 230 feet (70 meters) were unavoidable. The spacing between wires of *SOJ* pairs was increased to 11.8 inches (30 centimeters) for these long spans only.

In selecting *S*-pole transpositions, all transposition sections of the same type within a main *SOJ* repeater section were considered as a series, regardless of the number of transposition sections of other types separating them.

Attenuation, far-end cross-talk, near-end cross-talk, and return-loss measurements were made on the *SOJ* pairs from each end of the repeater sections from Cachoeira Paulista to Caçapava and from Caçapava to Tatuapé in December, 1948, and January, 1949, respectively.

TABLE 5
FAR-END CROSS-TALK-RATIO PEAKS

Between Places	Between Pairs	Cross-Talk-Ratio Peaks in Decibels	
		36-84 Kilocycles	92-143 Kilocycles
Cachoeira and Caçapava	Adjacent	66	58
	Alternate	69	59
	Outside	71	65
Caçapava and Tatuapé	Adjacent	66	57
	Alternate	68	58
	Outside	76	66

Analyses of the far-end cross-talk-ratio curves on all permutations of the four *SOJ* pairs measured from each end of the repeater sections showed no peaks worse than those given in Table 5.

A more detailed analysis showed that these repeater sections were well within the limits set in Section 2.2.

Typical cross-talk results for the section from Caçapava to Tatuapé are shown in Figure 9.

The attenuation curves showed no absorption peaks greater than 0.003 decibel per mile. A typical result is shown in Figure 7. The return-loss measurements (made with pure resistances) were

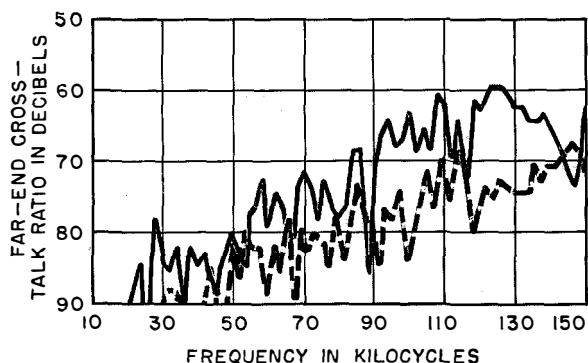


Figure 9—Typical far-end cross-talk-ratio curves for the J-5-transposed circuits between Caçapava and Tatuapé, a distance of 79 miles (127 kilometers). The solid line is for pair 7-8 disturbing and 3-4 disturbed. The broken line is for pair 9-10 disturbing and 1-2 disturbed.

best when the line was terminated at the far end in 550 ohms and its impedance compared with 550 ohms, in which case all pairs gave a return loss between 5 and 150 kilocycles of better than 29 decibels.

Further tests were made later between Caçapava and Tatuapé to confirm that cross talk

between the zero arm and the first, third, and fifth arms was satisfactory at *C* frequencies. The results showed no far-end cross-talk-ratio measurements with the zero arm worse than 60 decibels up to 30 kilocycles, and the vast majority much better. They also showed that a pair could be chosen with satisfactory cross talk to the zero arm for operation of an additional suitably staggered *SOJ* system on a manual-gain-control basis.

5.5 INTERACTION CROSS-TALK SUPPRESSION

In this type of 12-channel carrier system, in which there is no frequency translation at repeater stations, quite low couplings between *SOJ* pairs and other pairs or the longitudinal of the line may cause high cross talk or even singing around a repeater station. As described elsewhere,⁶ this is controlled by cutting a gap in the

⁶ See pages 376 and 377 of reference 5.

Figure 10—Cachoeira Paulista repeater station. The “old” line to Barra Mansa is on the left with its new spur line from the Caçapava side terminating on the pole (shown up close in Figure 11) beside the building in the center of the picture. The terminal pole on the Bananal side is to the right in the background. The “gap” between the terminal poles on either side of the station can be seen clearly.



line in front of the repeater station, installing cross-talk-suppression filters on non-*SOJ* circuits passing through the station, and installing longitudinal choke coils on all circuits entering the station.

In the cases of Bananal and Cachoeira Paulista, the suppression was quite simple and standard, since few circuits were involved and the necessary gap was easily established. In the latter case, since it was not desirable to lead in the circuits of the existing line passing on to Barra Mansa, a project to connect the town of Cachoeira Paulista direct to a point on the line to Barra Mansa instead of passing through the repeater station was dropped since interaction cross-talk paths would be established around the triangle so formed. Details are illustrated in the photographs in Figures 10 and 11.

The case of Caçapava was far more complicated. A gap had already been established of about 55 feet (16.8 meters). The existing toll circuits entered the station from the terminal poles on either side of this gap, running in separate cables to the toll distributing frame.

The existing subscribers circuits were taken off from poles about 1400 feet (427 meters) away (Rio de Janeiro side) and 2400 feet (732 meters) away (São Paulo side), where they entered cables that were strung on the pole route to the two terminal poles outside the station, whence they entered a cable chamber in separate cables. These cables were spliced into cables common to all subscribers and thus ran to a main frame in the switchboard room. On the Rio de Janeiro side, there were 14 subscribers pairs on the open-wire line, the longest running on it for about 4 miles (6.4 kilometers); on the São Paulo side there were 8, the longest running for about 6 miles (9.7 kilometers).

A condition was thus possible whereby an open-wire-line subscriber on one side being connected through to one on the other side of the station, the gap would be effectively bridged. There were some toll circuits also that passed directly through the station without voice-frequency repeaters as well as some passing through repeatered. In addition, tests made on the existing 3-channel carrier repeaters showed that the attenuation through them in the *B-A* direction was quite low even at 140 kilocycles (in some cases only about 10 decibels).

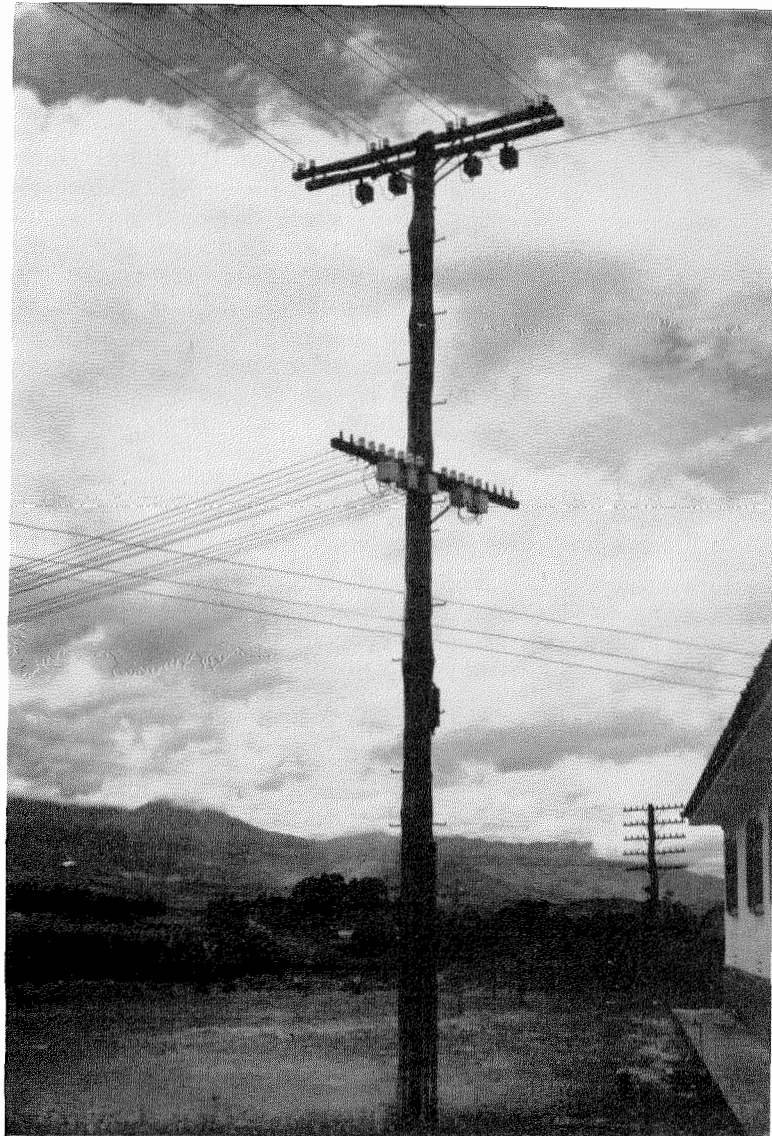


Figure 11—Terminal pole on the Caçapava side of the Cachoeira Paulista repeater station. The circuits on the lower crossarm enter the station to connect to interaction cross-talk-suppression filters. The boxes on the crossarms contain carbon arresters and longitudinal choke coils to assist in suppressing interaction cross talk around the station.

The voice-frequency repeaters were all equipped with low-pass filters, but the coupling in the wiring backwards and forwards between the toll test board, repeating coils, etc. was an unknown factor. The following suppression plan was therefore adopted.

- A. The gap of about 55 feet (16.8 meters) was maintained.
- B. Longitudinal choke coils were installed in all open-wire toll and subscribers circuits on both sides of the station.

C. All open-wire circuits from the Rio de Janeiro side of the station were connected to cross-talk-suppression arrangements before coupling was possible with other circuits. In the case of 3-channel carrier repeaters, "roof" filters were connected in the *B-A* direction and the jumpers on the toll distributing frame on the *B* side were run in screened pairs. In the case of all through nonrepeated circuits, through repeated circuits on the first 4 crossarms, terminated circuits from the Rio de Janeiro side, and open-wire subscribers' circuits on the Rio de Janeiro side, 12-kilocycle cross-talk-suppression filters were equipped and connected by screened jumpers on the Rio de Janeiro side.

D. For leading in the subscribers circuits on the Rio de Janeiro side, a new 26-pair cable was spliced in to lead the open-wire circuits concerned direct to the toll distributing frame.

As described later, these arrangements appear to have been successful in eliminating interaction cross talk.

5.6 LINE-CONSTRUCTION DETAILS

In general, the Companhia Telefonica Brasileira aims at attaining International Telephone and Telegraph System standards of line construction, and most of the dimensions of the open-wire pole-route-line materials are based on those of that organization, modified to fit in with the metric system.



Figure 12—Typical crossarms, insulators, and transposition brackets. The zero crossarm carries 5.9-inch (15-centimeter) spaced wires on type-2 porcelain insulators mounted on *H-15*-type transposition brackets. The first crossarm supports wires with 11.8-inch (30-centimeter) spacings; they are carried on double-petticoat alkaline-glass insulators mounted on both point- and drop-type transposition brackets.

The standard crossarm for toll circuits until the late thirties was the 3-meter (about 9-foot 10-inch) type with 30-centimeter (about 11.8-inch) spacing between wires as shown in Figure 3A. Later, this crossarm was modified to give 20 centimeters (about 7.9 inches) between wires

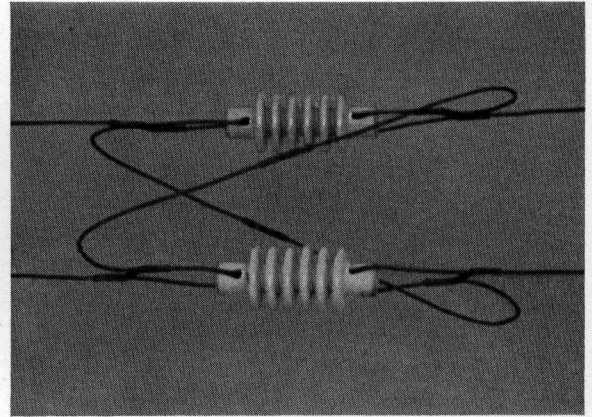


Figure 13—Special suspended-type transposition arrangement used to a limited extent on very long spans.

for use on carrier transposed pairs, as shown in Figure 3C and the 18-pin crossarm shown in Figure 3B was introduced on some routes to increase their circuit-carrying capacities. For the *SOJ* project, the 8-pin crossarms shown in Figure 3D and 3E were introduced to give 20-centimeter (about 7.9-inch) and 15-centimeter (about 5.9-inch) wire spacings. The crossarms are almost invariably wooden. Typical crossarms are shown in Figure 12.

Drop-type transposition brackets are generally used on voice-frequency transposed wires and point-type on carrier transposed wires. The point-type was, previous to 1947, made up of two separate plates each mounting two pins with insulators and kinked so as to give the necessary wire clearance at the point of crossover. For the *SOJ* project two *H* types were developed for the 7.9-inch (20-centimeter) and 5.9-inch

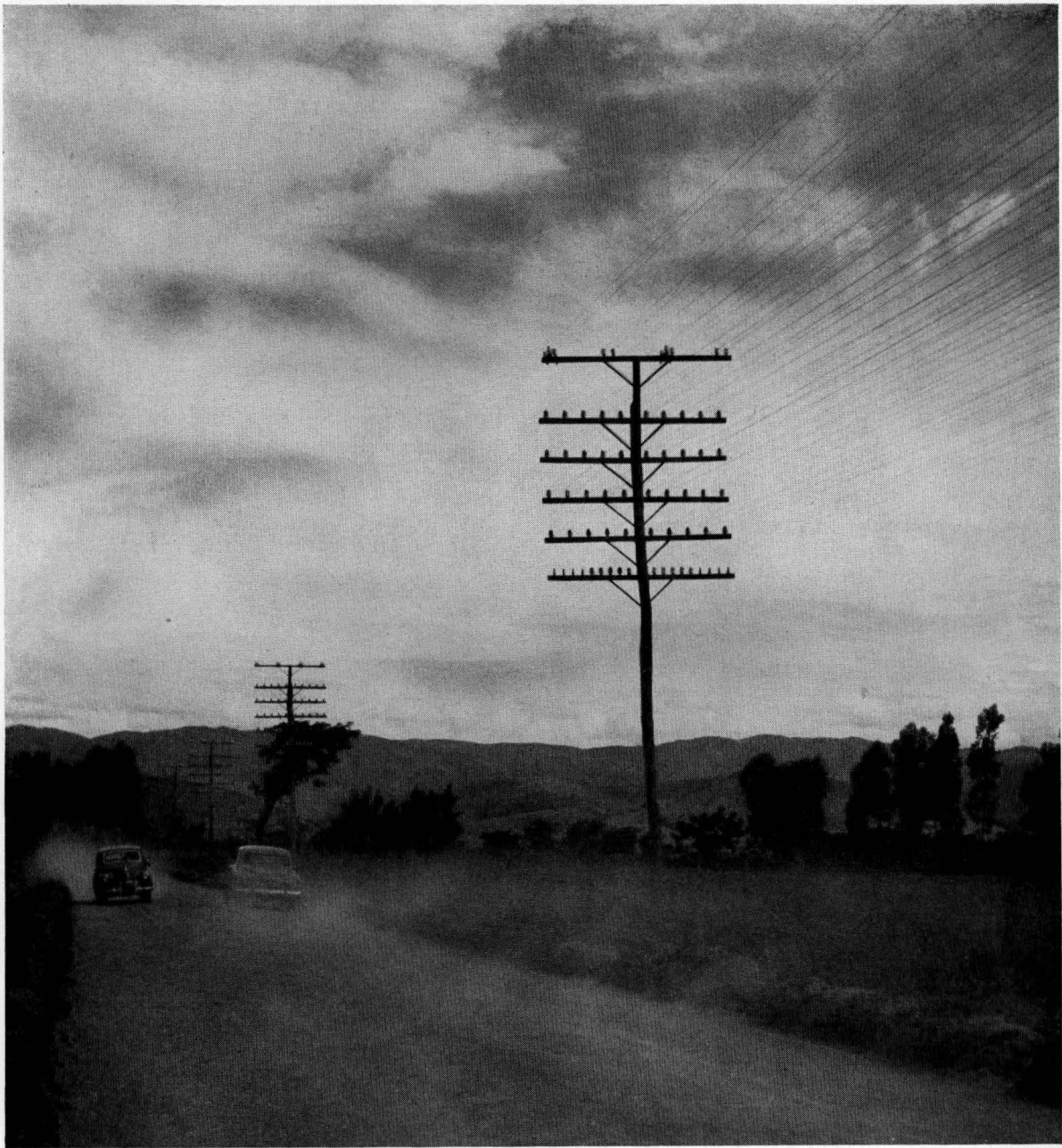


Figure 14—A few poles in the line between Cachoeira Paulista and Caçapava.
The typical dusty road conditions are evident.

(15-centimeter) wire spacings, respectively. Several types are shown in Figure 12.

In two places, it was impossible to locate poles on which to install transpositions and, since by so doing a great improvement could be effected in the transposition-point-spacing deviations (as described in Section 5.4 above), it was decided to

install a suspended type of transposition arrangement shown in Figure 13. This was to be installed on the *SOJ* pairs only, since the pole-spacing-deviation limits for the other pairs would be met in any case. For this purpose, a special insulator was designed about $4\frac{3}{4}$ inches (12 centimeters) long by about 1 inch (2.5 centimeters) basic

diameter with holes through which to pass the wires and 6 concentric ribs 2 inches (5 centimeters) in diameter. The wires from each side were terminated on a pair of these insulators and jumpers connected to make the crossover, as shown in Figure 13. Since these were only

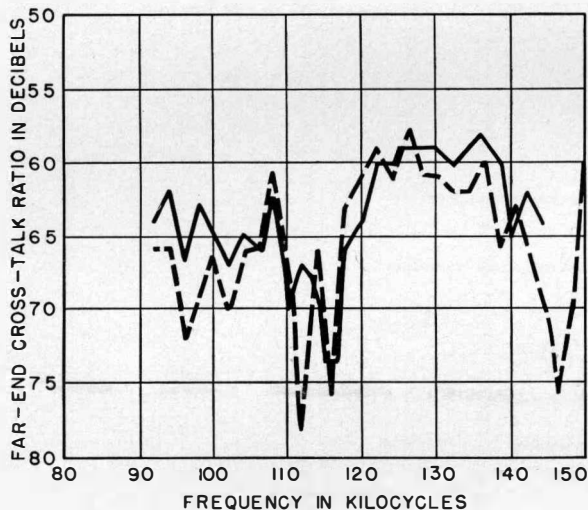


Figure 15—Typical comparison of far-end cross-talk ratio with (solid line) and without (broken line) lead-in cables. These values are for the section between Tatuapé and Caçapava for pair 03-04 disturbing and 01-02 disturbed.

required to be used in exceptional cases (two on this project), the leakage was not considered of great importance and the installation costs would be negligible.

Double-petticoat alkaline-glass insulators imported from the United States have been used on toll circuits extensively in the past, but Brazilian porcelain is reputed to be among the best in the world and the type-2 porcelain insulator developed in Brazil is now standard for the Company's toll circuits. Both types are shown in Figure 12.

The vast majority of the poles used are of Aroeira wood—the hardest of the hard Brazilian woods. These poles often are not straight, but, despite this, the cross-arm spacing and symmetry of arrangement obtained in practice is as good as is generally obtained with poles that are quite straight. In towns, cement or steel (tram-rail) poles are generally used.

The *SOJ* open-wire pairs are in every case led in from the terminal poles direct to the line filter bays by means of low-capacitance cotopa-

spaced paper-insulated quads of the *T.C.S. 314* type supplied by Standard Telephones and Cables, Limited. Protection is provided on the poles in the same box as the longitudinal choke coils and consists of the *26/30*-type carbon arresters (breakdown voltage around 750). On the line filter bays, *26/27*-type carbon arresters (breakdown voltage around 350) are supplied, which are followed by variable-resistance elements called "Metrosil discs," which have a low resistance when high voltages are applied across them.

Variable loading units are provided on the line-filter end of the lead-in cables; these were adjusted to give the optimum impedance match at the junction of cable with open-wire line when measured as a return loss.

6. Over-All Cross-Talk and Noise Results

6.1 GENERAL

An inspection of the cross-talk results on individual repeater sections indicated that *SOJ* systems types *A*, *B*, *C*, and *D* would give the best intersystem cross talk if operated over the whole length of the line on pairs 1-2 (01-02), 3-4 (03-04), 7-8 (07-08), and 9-10 (09-010), respectively. They were accordingly so connected for the final tests.

By August 1949, the line-up had been completed on most of the channels of three systems and on the high-frequency side of all four systems in the *A-B* direction. The circuits were urgently required for traffic, but, before they were handed over, certain cross-talk and noise tests were made to ascertain to what extent the planning had been effective.

Later, when a total of 45 channels had been lined up, more extensive cross-talk and noise measurements were made at nighttime.

The main object of these tests was, of course, to confirm as far as possible that the cross talk and noise on the channels at all normal times was such that the high quality of transmission provided by the *SOJ* channels in other respects was not impaired. Secondary objectives were:

A. To ascertain to what extent the tentative high-frequency line cross-talk limits given in Table 1 correlated with the intersystem cross talk when measured as noise on the channels.

B. To confirm that the lead-in arrangements properly matched the impedance of the equipment to that of the open-wire line.

C. To confirm that the interaction cross-talk suppression at repeater stations was effective.

D. To observe in what way the cross talk on repeater sections added up in practice.

E. To obtain information regarding the pure line noise.

6.2 HIGH-FREQUENCY CROSS TALK

The carrier-frequency line cross-talk measurements included the lead-in cables, line filters, and, in the case of Nova Iguazú, the entrance cable with its associated matching arrangements. Far-end cross-talk measurements were first made in the *A-B* direction on each repeater section and then on two or more repeater sections with

similar measurements were made in the *B-A* direction.

The results of the measurements made on each repeater section were plotted on the same paper as those obtained nearly a year earlier on the open-wire only (except for the Bananal-Nova

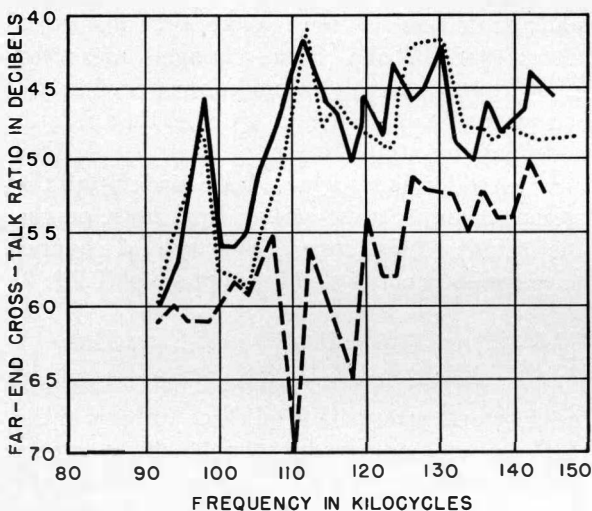


Figure 16—The over-all far-end cross-talk ratios for the complete circuit from Tatuapé to Nova Iguazú are shown by the solid line. The broken line is for the Tatuapé-Banal section. The remaining section from Bananal to Nova Iguazú, shown dotted, comprises about a quarter of the total circuit length but contributes dominantly to the cross talk. Measurements were made with repeaters lined up for pairs 03-04 (3-4) disturbing and 01-02 (1-2) disturbed.

repeaters properly lined up, but operating on a manual-gain-control basis, between Tatuapé and Cachoeira Paulista, Bananal, and Nova Iguazú, in turn.

Later, the over-all measurements between Tatuapé and Nova Iguazú were repeated and

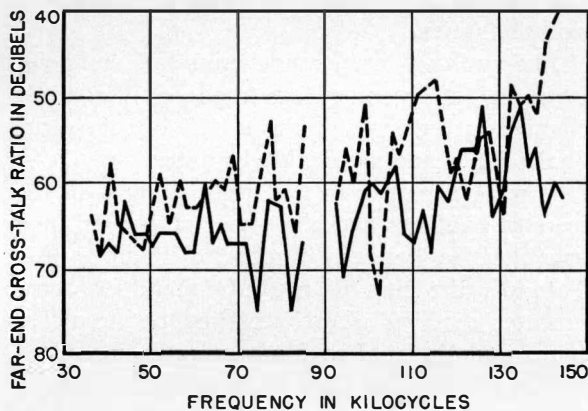


Figure 17—Typical over-all high-frequency cross-talk ratios with repeaters lined up for the Tatuapé-Nova Iguazú circuit. The solid line is for system *A* disturbing and *D* disturbed. The broken line, for *B* disturbing and *C* disturbed.

Iguazú section for which no previous test results were available). The curves were generally about the same shape and the peaks seldom differed by more than 2 or 3 decibels. A typical result is shown in Figure 15.

These results were regarded as practical proof that the impedance matching of lead-in cable with open-wire line had been made satisfactorily.

Analyses of the results of the other measurements led to the following conclusions.

A. In general, the cross talk appeared to add up as the sum of the powers present, although there were notable exceptions. No cases were found in which the sum was more than 6 decibels worse than either component and few in which it was more than 2 or 3 decibels worse.

B. The repeater section between Bananal and Nova Iguazú was undoubtedly the controlling factor in the over-all cross talk in every case. This is well illustrated in Figure 16, which is a typical result.

C. Interaction cross talk was negligible at repeater stations under the conditions of the tests.

Figure 17 shows typical over-all high-frequency cross-talk results between Tatuapé and Nova Iguazú. An analysis of results is given in

Table 6, from which it will be seen that, with one exception, they are within the limits tentatively set in Section 2.2. Many of them are just on the limit so that the method of interpretation of the results and the exact staggering advantages assumed are found to tip the balance between a fair proportion of the results being within or outside the limits.

The results of interchannel cross-talk and noise tests and of listening tests made on the worst channels at heavy-traffic times are of course the final criteria and are dealt with later.

It was gratifying to find that, despite all the fears of conflicts and the effect of pole-spacing irregularities between Cachoeira Paulista and Tatuapé, the sum of the cross talk for three repeater sections when measured between Tatuapé and Bananal with repeaters lined up was well within the tentative limits set in Section 2.2 for a single repeater section. In fact, it was so well within limits that the Bananal-to-Nova Iguaçu section could be allowed to contribute practically all the over-all high-frequency cross talk and thus, although it was outside the limits set for a single section, the over-all cross talk was within the tentative limit.

6.3 INTERCHANNEL CROSS TALK AND NOISE

These measurements were made between Nova Iguaçu and Tatuapé with all channels lined up to 3.5 ± 0.5 decibels loss between the 2-wire points; with this line up, the system levels were approximately the same as for the final line up between Rio de Janeiro and São Paulo with the entrances to the two cities connected on a 4-wire basis. The tests included A) channel noise, B)

TABLE 6
OVER-ALL FAR-END CROSS-TALK RATIO BETWEEN
TATUAPÉ AND NOVA IGUAÇU WITH
REPEATERS LINED UP

Combination of SOJ Systems	Maximum Peaks in Decibels			
	Results		Limits	
	B-A	A-B	B-A	A-B
A and B	50	40	47	40
A and C	62	47	53	46
A and D	60	51	47	40
B and C	53	40	47	40
B and D	55	45	53	46
C and D	55	44	47	40

within-system interchannel cross talk, and C) intersystem interchannel cross talk.

6.3.1 Channel Noise

The channel noise measurements were made at the same time as the intersystem measurements with all channels of the four systems properly terminated and with no disturbers connected. The measurements were made with a Western Electric 2-B Noise-Measuring Set using F-1-A weighting and the results expressed in decibels adjusted (dba).

To prove that the line noise is within limits, a prolonged series of measurements under all types of weather conditions is necessary, and this has not yet been done. However, under the conditions prevalent during several series of tests, including very heavy dew, which on this line appears to correspond approximately with wet weather as far as line attenuation is concerned, many channels in both directions measured better than 18 dba. Some channels measured worse, due apparently to noise introduced in the equipment in Tatuapé, a trouble that is still under investigation.

Thus, so far as tests have been made up to the present, channel noise arising from noise on the line is quite satisfactory. Some typical channel noise results are included in column 3 of Table 7.

6.3.2 Within-System Interchannel Cross Talk

The within-system interchannel cross-talk measurements were made on three systems in the A-B direction by speaking on 11 channels of a system and measuring at the far-end on the remaining channel with a 2-B Noise-Measuring Set. The results showed that this type of cross talk was negligible and no further measurements of it were made.

6.3.3 Intersystem Interchannel Cross Talk

To measure the intersystem cross talk in such a way that other channel noise had a negligible masking effect, the conditions for these tests were purposely made considerably more severe than those under which the channels would be used in practice.

All channels on all four systems were terminated at the 2-wire point in 600 ohms at both ends; the 2-B Noise-Measuring Set was con-

nected to the disturbed channel in place of the termination at one end and the noise measured on the channel without any disturbers. Magneto-type telephone sets equipped with Western Electric *F-2A* capsules were then connected at the other end in place of the terminations on all channels whose frequency bands overlapped that of the disturbed channel. The speakers disturbed first on one system at a time and then on all three systems at the same time. They were male voices adjusted so that a Western Electric volume meter⁷ indicated about +4 volume units on peaks when bridged across the circuits.

Having decided to establish these test conditions the difficulty arose as to how the results could be related to the practical case of traffic on the circuits.

Several factors had to be taken into account. Among the more important were the relation between the circuit levels during the tests and in the final line-up and the relation between a number of disturbers speaking at a fairly con-

⁷ The type of volume indicator used is calibrated to indicate 0 volume units when it is bridged across a 600-ohm circuit with 1000 cycles at 0 decibels relative to 1 milliwatt.

stant volume of +4 volume units and the conditions to be expected in practice with two-way conversations between subscribers with voices, loops, and telephones that might be very different from those of the test. After consideration of these and other factors, it was decided that the conditions could be considered to be approximately 13 decibels more severe than the worst that would be encountered in practice. It was therefore decided to regard cross talk as outside limits when it gave rise during these tests to channel noise worse than 38 decibels adjusted.

The results showed that on the 45 channels tested all channels in both directions were within this limit, except for channel 3 of system *D* in the *A-B* direction, which measured 39 dba; in addition, it was not possible to measure cross talk within limits on 4 channels owing to noise introduced in Tatuapé being worse than 38 dba.

To illustrate the relation between the high-frequency cross talk on the line and the inter-system cross talk on the channels, Table 7 has been prepared for all channels in the *A-B* direction into which cross talk introduced noise that measured worse than 33 dba.

TABLE 7
INTERSYSTEM CROSS TALK IN *A-B* DIRECTION SHOWING RESULTS ON WORST CHANNELS

Disturbed		Measured Channel Noise in dba						Approximate High-Frequency Line Cross Talk in Decibels from System			
		Without Disturbers	With Disturbers on Systems								
System	Channel		A	B	C	D	All 3	A	B	C	D
A	1	18	—	32	26	22	35	—	(40)	(46)	(40)
	2	17	—	24	30	21	38	—	43-44	52-53	58-66
	3	17	—	36	25	21	37	—	44-45	55-62	52-53
	4	15	—	35	24	19	36	—	42-43	59-60	57-58
	7	17	—	32	32	21	34	—	44-45	56-60	58-62
	8	18	—	37	28	18	37	—	43-44	52-55	56-63
B	1	15	26	—	19	27	34	(40)	—	(40)	(46)
	3	19	32	—	30	27	34	42-46	—	53-57	52-57
	5	15	27	—	26	34	35	49-50	—	46-48	52-57
	6	15	30	—	26	36	37	44-60	—	53-57	52-56
	7	28	35	—	29	32	37	40-46	—	49-50	52-55
	9	15	26	—	19	32	34	40-42	—	54-56	51-58
C	4	15	28	27	—	24	36	(46)	(40)	—	(40)
								56-59	56-58	44-52	
D	3	22	27	37	28	—	39	(40)	(46)	(40)	—
	4	19	22	35	20	—	35	52-59	45-49	46-47	—
	5	20	24	34	21	—	36	55-64	47-50	46-47	—
	8	22	22	28	22	—	35	53-57	50-60	47-53	—
								63-67	47-57	52-55	—

Note: Figures in parenthesis are the limits set in Section 2.2.

In examining Table 7, it is advisable to bear in mind how difficult it is to control accurately the sending volume in cross-talk tests of this type. One can picture a hot repeater station in the early hours of the morning; five telephones are arranged round a table with their speakers. On a word from the controller, two men lift their receivers and speak into the microphones, the controller urging them to regulate their outputs according to the readings on the volume indicator that he can connect across any circuit. On advice from the far-end, another pair speak, then one speaks alone, and then all five speak together. In the meantime, coffee has been prepared and, in the next series of measurements, voices can be expected to be louder.

It is surprising, in the circumstances, to find on examining Table 7 that it is generally from precisely those channels where the high-frequency line cross talk is nearest the limit that a channel receives noise nearest the 38 dba limit. An examination of the table indicates that the channels with the 46-decibel high-frequency cross-talk limit tend to disturb a little more than would be expected, but, on the whole, the line cross-talk limits appear to be about correct.

The fact that the only channel outside limits corresponded with the only high-frequency result outside limits is interesting but can only be regarded as a general trend rather than positive proof of a rigid relationship between the two sets of measurements. In another series of these tests in which many results were so near the limits for both high-frequency cross talk and channel noise and the test conditions were so difficult to control, other channel combinations might be found to be just outside limits.

The real criterion, of course, is whether or not the cross talk is of such a magnitude that it interferes unduly with the exchange of information over the channels by means of speech. Some listening tests were made that indicated that, even during the busy hour, the cross talk did not appreciably interfere with speech, although it could be clearly heard.

However, it would be wise to expect the cross-talk condition effectively to worsen as the general toll service improves and the subscribers become more critical and hence more easily

annoyed by cross talk and also as the operating methods and facilities improve so that more conversations are in progress simultaneously on the channels.

7. Conclusions

A. The construction and transposition of the open-wire line are such that intersystem cross talk is at a satisfactorily low level for the present conditions.

B. This result was reached only by obtaining a superior performance on more than three quarters of the line to permit the remainder to contribute nearly all the over-all cross talk.

C. Conclusive evidence has not yet been obtained that the repeater-station spacing, gage of wire, and transposition systems employed give satisfactory channel noise derived from pure line noise under all normal weather conditions. However, the tests detailed here and others not mentioned indicated that this part of the planning also had been satisfactory.

D. The test results obtained on the 140 miles (225 kilometers) of line on which the extension arm was erected showed that a very satisfactory performance had been obtained.

E. The use of human speakers in multiple-disturber cross-talk tests in which the measurements are made in terms of noise is not very satisfactory. Some means of producing artificial speech from 11 outputs with the necessary random distribution is very desirable for this type of work.

F. The application of four additional *SOJ* systems to the line can be expected to present some interesting problems. Between Km 117 and Cachoeira Paulista, the installation of the second arm will provide a simple solution. Between Cachoeira Paulista and Tatuapé, it may prove economical to construct a new line along the new road that is now nearing completion; on the other hand, it may be decided to retranspose the existing second crossarm [5 feet (1.5 meters) below the zero arm] to the *J-5* second- or third-arm arrangement. Between Nova Iguaçu and Km 117, the solution of the problem will depend to some extent on whether or not it is decided again to allow this part of the line to contribute nearly all the total cross talk. The use of compandors will also have to be considered when applying further *SOJ* systems to the line.

G. In tackling a problem of the type outlined in this article, the engineer has to choose constantly between a costly plan that will certainly give the required technical result and one that may give a borderline result but which will save a great deal of money if successful. He has to remember that the whole object of the project is to provide the additional toll service economically, a fact that in practice he is unlikely to be allowed to forget for long. Retransposing or stringing new wire and relocating poles is a costly business, but, if the engineer departs from standard practice, as he must do in a case like this, and if he relaxes on the normal limits, then he will know whether or not his planning has been successful only when the tests are made on completion of the work; if it has not been successful, then the whole program may be upset and the final result far more costly than would have been the case if the right plan had been followed in the first place. The proper presentation of a technical plan to nontechnical commercial and financial staff and an understanding of their problems, the successful solution of which keeps the company in business, become essential parts of the engineer's job in this type of work.

H. Experience plays an important part in finding an economical solution to this type of problem.

8. Acknowledgments

The author expresses his appreciation to all those who assisted both directly and indirectly in the production of this article, to Mr. L. H. Armstrong, Transmission Engineer of the Companhia Telephonica Brasileira, for his advice and encouragement and to his colleagues Messrs. A. W. Ewen, G. H. Foot, P. F. Webb, I. Kristiansen, J. Padlas Jr., C. Romeu, and many others who collaborated in the work on which the article is based.

Recent Telecommunication Development

Television Transmitting Antenna for 174-216-Megacycle Band

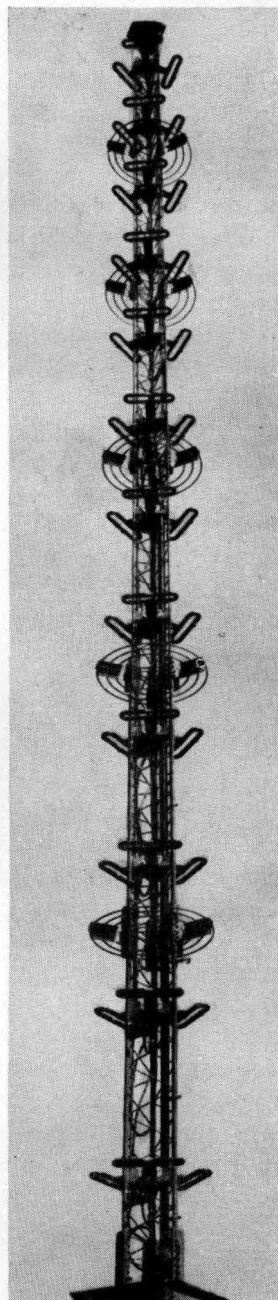
TELEVISION BROADCASTING, utilizing dominantly line-of-sight propagation for its primary coverage, requires a transmitting antenna producing in the horizontal plane a uniform circular distribution of radiation and in the vertical plane a highly concentrated pattern aimed toward the horizon.

The antenna shown consists of 12 triangular loops or bays. Each loop, consisting of three folded dipoles, can safely handle a kilowatt of power and radiates both the visual and aural signals.

The 12-bay antenna has a power gain of 11.8, equivalent to 10.7 decibels, over that of a half-wave dipole in the direction of the horizon. Up to 16 bays can be used to give power gains of 15.4 (11.9 decibels) and produce fields of effective radiated powers exceeding 240 kilowatts.

The same tower structure can be used for any channel in the television broadcasting band extending from 174 to 216 megacycles per second.

In Buenos Aires, an 8-bay antenna and 5-kilowatt transmitter built by Federal Telecommunication Laboratories produces the highest effective radiated power (45 kilowatts) of any television station in the Americas.



Determination of the Piezoelectric Constants of Some Isomorphous Crystals*

By F. P. SPITZER

Standard Elektrizitäts-Gesellschaft A. G., Stuttgart, Germany

QUANTITATIVE investigation of the piezoelectric activity of crystals, especially of those that may be artificially grown from organic or inorganic substances, has made but small progress since the fundamental research done by Voigt, Riecke, Pockels, and their pupils. Only quartz and Rochelle salt were repeatedly investigated with respect to their technical characteristics.

The click method of Giebe and Scheibe has been valuable for testing qualitatively the piezoelectric activity of crystalline substances and has allowed rough conclusions to be drawn with respect to the intensity of the effect. With the help of this method, many substances have been investigated, especially by Hettich, in a search for materials having piezoelectric properties. A number of substances having strong piezoelectric activity have been found. Later, quantitative determination was made of the piezoelectric effects of such organic compounds as rhamnose, hexamethylene tetramine, and asparagine by Meyer and Gockel.

This paper is concerned with a continuation of this search for substances having a positive Giebe-Scheibe effect and the determination of the piezoelectric constants of those that show this effect to a high degree. The search for suitable substances having strong piezoelectric effects is well justified by the fact that quartz and Rochelle salt crystals, used hitherto exclusively for technical purposes, are not adequate for all possible applications.

Extensive investigations of similar substances and a comparison of the findings is of aid in understanding the electrophysical properties of crystals. Only a few investigations of a quantitative character have been carried out in this direction. Valesk observed the temperature relation of the piezo effect of sodium bromate and has compared the results with the behavior of

* This is a translation of part of an unpublished thesis accepted by the University of Göttingen in 1938.

sodium chlorate, while Mandell investigated ammonium Rochelle salt in view of the strong piezo effect of sodium potassium tartrate.

By the Giebe-Scheibe method, substances having large piezoelectric effects may be identified. As a result of such preliminary tests, the primary phosphates of potassium and ammonium, nickel sulphate hexahydrate, lithium sulphate, potassium tartrate, ammonium tartrate, ammonium oxalate, strontium formate, and barium formate appeared promising. Likewise the isomorphous substances, sodium chlorate and sodium bromate, as well as heptahydrates of zinc sulphate, magnesium sulphate, and nickel sulphate appeared promising.

1. Growing of Crystals

The chief difficulty that had to be overcome was the manufacture of suitable specimens of the selected substances. Attempts to grow suitable crystals of ammonium oxalate, strontium formate, and barium formate did not lead to satisfactory results although the Giebe-Schiebe effect looked promising at least for the first two compounds. In the case of the other substances, the growing of crystals was accomplished by cooling or evaporating the solvent from a saturated aqueous solution in which a seed was placed. The growth was effected in equipment of the type described by Moore and Schwartz.

The temperature of crystallization was between 30 and 40 degrees centigrade except for the crystallization of nickel sulphate. The crystallization of rhombic nickel sulphate was effected at 20 degrees centigrade as this form is produced only below 30 degrees. After some preliminary tests to determine suitable growing conditions, the growth of the following crystals was successfully accomplished: NaBrO_3 , KH_2PO_4 , $\text{NH}_4\text{H}_2\text{PO}_4$, $\text{NiSO}_4 + 6\text{H}_2\text{O}$, $\text{NiSO}_4 + 7\text{H}_2\text{O}$, $\text{ZnSO}_4 + 7\text{H}_2\text{O}$, $\text{MgSO}_4 + 7\text{H}_2\text{O}$, and $\text{C}_4\text{H}_4\text{O}_6\text{K}_2 + \frac{1}{2}\text{H}_2\text{O}$. Greater difficulty was experienced in growing suitable lithium sulphate

and ammonium tartrate crystals. Lithium sulphate grows in plate form in the plane of $s(\bar{1}01)$ while ammonium tartrate shows prisms elongated in the b axis and thin vertically to a (100) . For investigation purposes, the thickness of the crystals has to be at least 10 millimeters. Therefore, the conditions had to be changed in such a manner as to get thicker crystals.

Following a proposal of Johnson, the seeds were fixed in a plane perpendicular to the b axis and rotated slowly in the solution.

Even seeds that were suspended vertically with respect to a or c and were left to themselves grew to become crystals of a considerable thickness by evaporation of the solvent. In this way, a lithium sulphate crystal was grown that reached 16 millimeters perpendicular to $(\bar{1}01)$ while an ammonium tartrate crystal grew to 19 millimeters perpendicular to a .

2. Processing of Crystals

The determination of the characteristic piezoelectric modulus requires the preparation of crystals in the form of rectangular parallelepipeds of certain orientation with respect to the crystallographic axis. To achieve a high degree of accuracy, the optical method of orientation of the crystal was used instead of the contact method. For this purpose, a reflection and a grinding goniometer, both capable of operating in azimuth and height were used. A well-grown crystal having good reflecting surfaces was glued on a support. The reflection goniometer is adjusted to suitably plane surfaces with known indices thus providing a basis for the calculation of those planes that have to be produced by grinding. Subsequently, the crystal support is transferred to the grinding goniometer and, after having set the calculated values of azimuth and height on both graduated dials, the limiting planes of the parallelepiped, which are perpendicular to each other, may be ground. The finishing is done by parallel grinding by hand on a tripod similar to the parallel grinder of Fues. The orientation of the reference system (x, y, z) corresponds to the crystallographic main axis (a, b, c) . In agreement with Voigt, Holman, and others, the twofold polar axis of monoclinic crystals coincides however with the z axis of the coordinate system.

3. Measurement of Piezoelectric Constants

The determination of the piezoelectric modulus consists in the measurement of that quantity of electricity that is generated by a known pressure on crystals of a given orientation. When the capacitance of the set-up is known, this measurement is reduced to the determination of the voltage to which this capacitance is brought by the quantity of electricity that is produced by the pressure.

To carry out this task, several methods may be used. However, the accuracy of the measurement may be impaired because of inadequate insulation. In principle, a loss of charge through insufficient insulation may be avoided by preventing any voltage drop from occurring between the electrodes of the crystal. Such a method has the advantage that the crystal is under well-defined conditions with respect to electric voltage stresses, since the field that arises through piezoelectric polarization is balanced by another field and the crystal is in an electrically neutral state during measurement.

If a crystal is subjected to a constant mechanical stress, it seems to be possible to determine the piezoelectric voltage by compensation. However, it must be noted that the adjustment of compensation forces requires time and is practicable only if a small voltage drop is admitted for the purpose of effecting a balance. Each voltage drop however, results in a loss of charge although it is small if the time constant of the whole system is large.

To avoid this source of loss, the mechanical stress should be a periodic function of time, thus causing the piezoelectric crystal to work as an alternating-voltage generator. If an alternating voltage of the same shape and opposite phase is applied to the piezoelectrically excited crystal, it may be kept continuously in an electrically neutral state. Each charge produced by the alternating pressure in the crystal is balanced or compensated instantaneously by an equal charge of opposite sign from outside. Equilibrium is effected by keeping a voltage indicator, which is in parallel to the crystal, continuously at zero. The execution of this idea may be carried out by the following measuring equipment.

The crystal that is to be measured is placed between two steel plates, the lower of which is

joined to a flexible membrane that is mechanically connected to the upper of two capacitor plates as may be seen in Figure 1. Both are loaded by a weight. On this static pressure is superposed an alternating pressure having a frequency of 1 cycle per second obtained by loading and releasing a spring. Thus, charges are generated on the crystal periodically and there are corresponding variations in the capacitance of the capacitor.

In Figure 2, a high-frequency oscillator is tuned primarily by $C1$, across which is the variable capacitor $C2$ associated with the crystal. The mechanical coupling between the upper plate of $C2$ and the crystal holder is indicated. The 1-cycle-per-second variation in the capacitance of $C2$ produces frequency modulation of the high-frequency output of the oscillator.

The frequency-modulated wave is impressed on a circuit tuned slightly off its center frequency so as to produce amplitude modulation through operation on the slope of the resonance curve of the tuned circuit.

A rectifier connected to the tuned circuit will show variations of rectified current that will

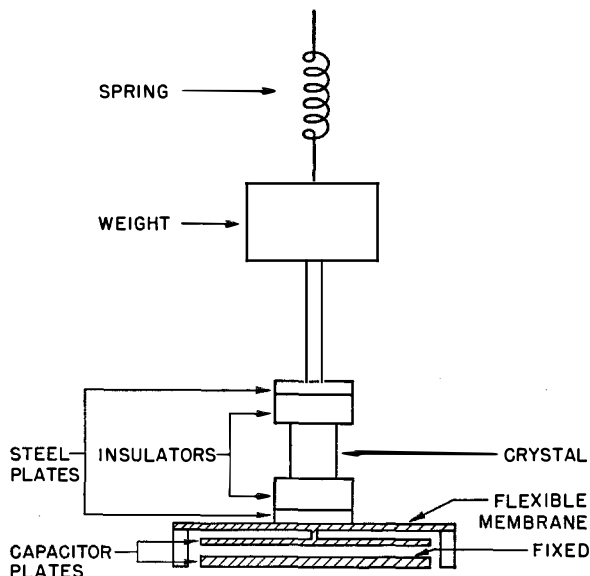


Figure 1—Crystal mounted on a capacitor having a flexible membrane joined to the upper plate. The weight and spring permit periodic variation of the pressure on the crystal and a corresponding variation in the capacitance of the capacitor. A suitable liquid bath maintains at constant temperature the housing in which the crystal and capacitor are mounted.

correspond exactly to the variations of the pressure applied to the crystal and its associated capacitor if the operating point is properly selected. A balancing arrangement suppresses the direct-current component while the alternating-current component generates an alternating voltage across a resistance. This alternating voltage is applied through a variable capacitor $C3$ to the piezoelectric crystal in such a manner that by adjusting its phase and amplitude no voltage exists across the crystal. A fast-acting reflecting galvanometer in the anode circuit of an electrometer tube may serve as a voltage indicator.

If a voltage e applied through $C3$ is required to balance exactly the alternating voltage generated by the crystal, and if e' is required for $C3+C3$, the maximum charge Q produced by a constant alternating pressure on the crystal is

$$Q = \frac{e e' C_3}{e - e'} \quad (1)$$

Therefore, we may write

$$\frac{Q}{C_3} = e$$

and

$$\frac{Q}{C_3 + C_3} = e'$$

If we put

$$e = i R \\ e' = i R',$$

where i is the amplitude of the rectified alternating current and R and R' are the resistances at which e and e' , respectively, are generated by i , we may write

$$Q = \frac{i R R' C_3}{R - R'} \quad (2)$$

In view of the fixed relation between the pressure applied to the crystal and the charge producing it, variations in the alternating current in the discriminator output circuit will be directly related to variations in the pressure on the crystal. The amplitude of the variation in pressure is given by (3).

$$p = \frac{i}{If}, \text{ kilograms} \cdot \text{centimeters}^{-2}, \quad (3)$$

where I represents the variation of current

resulting from a variation of 1 kilogram in the mechanical load and f is the area under compression. By combining (2) and (3) and after division by the metalized plated area F , the constant is determined by

$$d_{ik} = \frac{RR' C_3 I f}{(R - R') F}, \text{ ampere-seconds} \cdot \text{kilograms}^{-1} \quad (4)$$

By applying the same variations of pressure to the crystal as well as to the generator of the balancing voltage, the amplitude of the applied oscillating pressure does not appear in the

investigated in both directions. The values show an average error of about 2 percent. Measurements on monoclinic crystals may be regarded as less accurate in view of the very small excitations that had to be measured. Their moduli are therefore less accurate. Since the piezoelectric behavior of monoclinic crystals is very complicated, their smaller moduli are of less importance. Therefore, the investigation of the three monoclinic substances selected was carried out only to determine the largest moduli of the crystals in question.

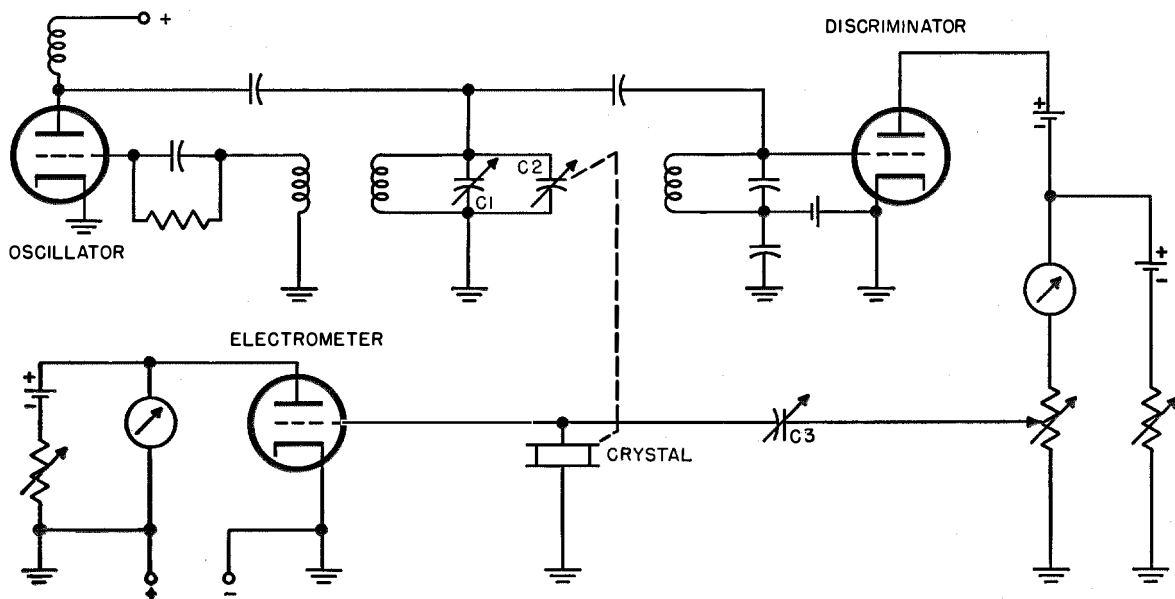


Figure 2—Circuit arrangement for testing crystals.

equation, provided that the voltages generated by the crystal and by the balancing equipment are proportional to the pressure.

For the determination of a modulus, two resistance measurements and one current measurement must be made. From the known variation of $C3$ and the dimensions of the crystal to be investigated, (4) may be used to calculate a value that, when multiplied by a factor according to the theory of Voigt, represents the modulus d_{ik} . This modulus is independent of any self-conductivity of the crystal. The observations have been carried out at a temperature of 20 degrees centigrade. The results are average values for several specimens. Where one specimen only was available, the crystal was in-

4. Results of Measurements

All of the modulus values given in this section are in electrostatic units per dyne.¹

4.1 QUARTZ

Two circular plates of quartz of equal diameter were cut perpendicular to the electric axis and arranged in such a manner that the longitudinal effects of the piezoelectric voltages created in both crystals were additive.

$$d_{11} = -6.93 \cdot 10^{-8}.$$

¹ To convert centimeter-gram-second electrostatic units to meter-kilogram-second (rationalized) units, use the conversion factor $\frac{1}{3} \times 10^{-4}$ coulomb/newton per statcoulomb/dyne.

Furthermore, a crystal already investigated by Voigt was available and was likewise excited longitudinally.

$$d_{11} = -6.94 \cdot 10^{-8}.$$

4.2 SODIUM CHLORATE

Since Meyer had found a modulus of NaClO_3 far higher than that given by Pockels, the modulus d_{14} was measured.

$$d_{14} = -5.23 \cdot 10^{-8}.$$

4.3 SODIUM BROMATE

$$\text{Specimen 1: } d_{14} = -7.23 \cdot 10^{-8}.$$

$$\text{Specimen 2: } d_{14} = -7.25 \cdot 10^{-8}$$

by transverse observation.

$$\text{Specimen 3: } d_{14} = -7.33 \cdot 10^{-8}$$

by longitudinal observation.

$$d_{14} = -7.27 \cdot 10^{-8}.$$

4.4 NICKEL SULPHATE HEXAHYDRATE

$$\text{Specimen 1: } d_{14} = -15.9 \cdot 10^{-8}.$$

$$\text{Specimen 2: } d_{14} = -16.0 \cdot 10^{-8}.$$

$$\text{Specimen 3: } d_{14} = -15.8 \cdot 10^{-8}$$

$$d_{14} = -15.9 \cdot 10^{-8}.$$

4.5 POTASSIUM PHOSPHATE

$$d_{14} = -3.85 \cdot 10^{-8}$$

$$d_{36} = -62.8 \cdot 10^{-8}.$$

4.6 AMMONIUM PHOSPHATE

$$d_{14} = +4.35 \cdot 10^{-8}.$$

$$\text{Specimen 1: } d_{36} = -137.5 \cdot 10^{-8}.$$

$$\text{Specimen 2: } d_{36} = -135.9 \cdot 10^{-8}$$

$$d_{36} = -136.7 \cdot 10^{-8}.$$

4.7 MAGNESIUM SULPHATE HEPTAHYDRATE

$$\text{Specimen 1: } d_{14} = -6.12 \cdot 10^{-8}.$$

$$\text{Specimen 2: } d_{14} = -6.25 \cdot 10^{-8}$$

$$d_{14} = -6.18 \cdot 10^{-8}$$

$$d_{25} = -8.16 \cdot 10^{-8}.$$

$$\text{Specimen 1: } d_{36} = -11.52 \cdot 10^{-8}.$$

$$\text{Specimen 2: } d_{36} = -11.48 \cdot 10^{-8}.$$

$$\text{Specimen 3: } d_{36} = -11.48 \cdot 10^{-8}$$

$$d_{36} = -11.5 \cdot 10^{-8}.$$

4.8 ZINC SULPHATE HEPTAHYDRATE

$$\text{Specimen 1: } d_{14} = -5.70 \cdot 10^{-8}.$$

$$\text{Specimen 2: } d_{14} = -5.69 \cdot 10^{-8}$$

$$d_{14} = -5.70 \cdot 10^{-8}.$$

$$\text{Specimen 1: } d_{25} = -10.5 \cdot 10^{-8}.$$

$$\text{Specimen 2: } d_{25} = -10.4 \cdot 10^{-8}$$

$$d_{25} = -10.5 \cdot 10^{-8}$$

$$d_{36} = -9.21 \cdot 10^{-8}.$$

4.9 NICKEL SULPHATE HEPTAHYDRATE

$$d_{14} = -5.98 \cdot 10^{-8}.$$

$$\text{Specimen 1: } d_{25} = -8.87 \cdot 10^{-8}.$$

$$\text{Specimen 2: } d_{25} = -8.80 \cdot 10^{-8}.$$

$$d_{25} = -8.84 \cdot 10^{-8}.$$

$$\text{Specimen 1: } d_{36} = -9.65 \cdot 10^{-8}.$$

$$\text{Specimen 2: } d_{36} = -9.60 \cdot 10^{-8}$$

$$d_{36} = -9.63 \cdot 10^{-8}.$$

4.10 LITHIUM SULPHATE MONOHYDRATE

$$d_{14} = +11.3 \cdot 10^{-8}$$

$$d_{15} = -12.0 \cdot 10^{-8}$$

$$d_{24} = -7.6 \cdot 10^{-8}$$

$$d_{25} = -2.9 \cdot 10^{-8}$$

$$d_{31} = -4.0 \cdot 10^{-8}$$

$$d_{32} = \text{very small}$$

$$d_{33} = +48.6 \cdot 10^{-8}$$

$$d_{36} = +19.8 \cdot 10^{-8}.$$

4.11 POTASSIUM TARTRATE HEMIHYDRATE

$$d_{14} = -19.7 \cdot 10^{-8}$$

$$d_{15} = -12.2 \cdot 10^{-8}$$

$$d_{24} = -34.6 \cdot 10^{-8}$$

$$d_{25} = -62.5 \cdot 10^{-8}$$

$$d_{31} = +2.3 \cdot 10^{-8}$$

$$d_{32} = +14.4 \cdot 10^{-8}$$

$$d_{33} = -14.6 \cdot 10^{-8}$$

$$d_{36} = +18.8 \cdot 10^{-8}.$$

4.12 AMMONIUM TARTRATE

$$d_{14} = +5.65 \cdot 10^{-8}$$

$$d_{15} = -14.0 \cdot 10^{-8}$$

$$d_{24} = -8.5 \cdot 10^{-8}$$

$$d_{25} = +9.3 \cdot 10^{-8}$$

$$d_{31} = +1.8 \cdot 10^{-8}$$

$$d_{32} = +17.6 \cdot 10^{-8}$$

$$d_{33} = -26.2 \cdot 10^{-8}$$

$$d_{36} = -5.9 \cdot 10^{-8}.$$

Behavior of Gas Discharge Plasma in High-Frequency Electromagnetic Fields*

By LADISLAS GOLDSTEIN and N. L. COHEN †

Federal Telecommunication Laboratories, Incorporated; Nutley, New Jersey

THE PURPOSE of this paper is to present the results of an experimental study of some of the properties of the gas discharge plasma. Specifically those properties were studied that are related to the complex conductivity of the gas discharge plasma, when placed in a high-frequency electromagnetic field. Two types of plasma have been investigated; A) the discharge plasma maintained by a direct-current field, and B) the disintegrating plasma obtained after excitation by a pulse of short duration.

It is known that the observable high-frequency phenomena in gas discharges are due to the interaction of the high-frequency fields with the electron gas that is supported by the plasma. To obtain a relatively high density of the electron gas in the plasma, it was desirable to utilize gases capable of supporting free electrons at all velocities. This requirement excluded the use of electronegative gases. As will be apparent, a further selection indicated that the use of gases having high first-excitation levels was preferable for this study. Therefore, the use of monatomic gases and particularly the rare gases was indicated.

The type of discharge used in most of the experiments was cylindrical, with both hot- and cold-cathode structures.

The gas tubes were inserted in a coaxial line to form a portion of the central conductor as shown schematically in Figure 1. Two experi-

ments were performed using a gas-filled rectangular waveguide so arranged that the discharge-tube electrodes did not interfere with the passage of high-frequency waves. In the coaxial-line experiments, the gas discharge tube was arranged so that the diameter of the visible plasma was approximately equal to the diameter of the inner conductor.

For the experiments, a high-frequency electromagnetic wave of the *TEM* mode was transmitted along the coaxial line. When there is no discharge, this wave is greatly attenuated by reflection due to the open section of the center conductor, since this region acts as a waveguide beyond cutoff. If a gas discharge plasma is established in the gap, however, and if the discharge plasma is conductive at the frequency

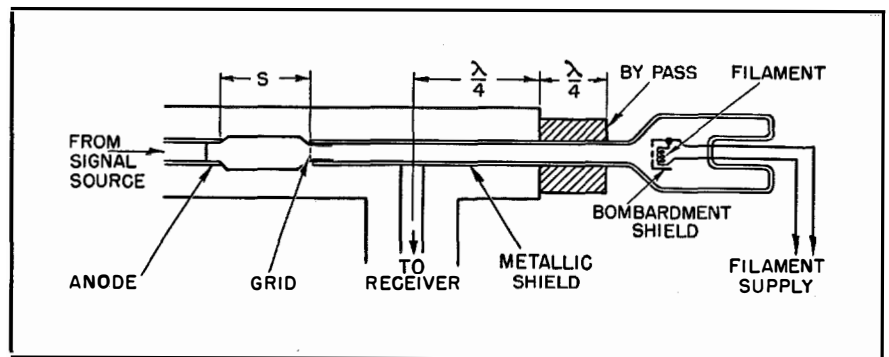


Figure 1—Coaxial gas discharge tube.

of the electromagnetic wave, the attenuation of the gap is reduced. In addition, the reflected radio-frequency signal is also reduced. The proportions between the reductions in attenuation and reflection may be used to determine the real and imaginary components of conductivity.

In the waveguide experiment with a radio-frequency signal, similar properties of signal reflection, attenuation, and phase-velocity changes should occur. In the case of the waveguide near cutoff, the phase velocity is a very

* This work was sponsored by the Air Material Command, Wright-Patterson Air Force Base, Dayton, Ohio.

† Now with Facsimile and Electronics Corporation, Passaic, New Jersey.

sensitive measure of the dielectric constant. The guide wavelength is given by

$$\lambda_g = \frac{\lambda}{\left[1 - \frac{1}{\epsilon} \left(\frac{\lambda}{\lambda_c}\right)^2\right]^{\frac{1}{2}}} \quad (1)$$

where

- λ = free-space wavelength
- λ_g = waveguide wavelength
- λ_c = cutoff wavelength for air dielectric
- ϵ = relative dielectric constant of plasma.

λ_g is plotted as a function of ϵ for $\lambda = \lambda_c/2$ in Figure 2, showing the sensitivity of λ_g -versus- ϵ characteristic for the case where the dielectric constant of the gas discharge plasma is entirely real.

These two types of complimentary experiments provide means to study the discharge plasma under two general conditions. The first, the coaxial-line experiment, aids study in the region of dielectric constants very much less than unity, and the second in the region of dielectric constants close to unity.

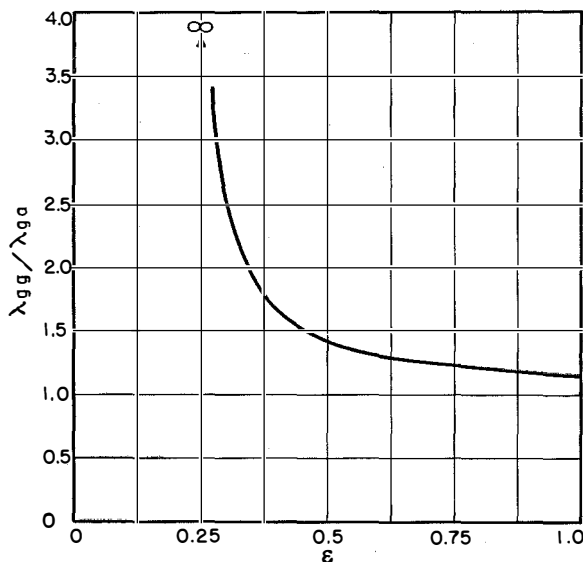


Figure 2—Waveguide wavelength plotted against dielectric constant of the gas discharge plasma $\lambda/\lambda_c = 1/2$.

$$\frac{\lambda_{gg}}{\lambda_{ga}} = \left\{ \frac{\epsilon_g [\epsilon_a - (\lambda/\lambda_c)^2]}{\epsilon_a [\epsilon_g - (\lambda/\lambda_c)^2]} \right\}^{\frac{1}{2}}$$

1. Experimental Setup

The experimental setup for the measurements is shown in Figure 3.

The generator¹ was variable in frequency from 1500 to 2300 megacycles per second and was provided with an attenuator calibrated in decibels with a nominal reference level of 20 milliwatts. Provision is made in the generator for either continuous-wave or pulse-modulated-wave output. In the pulse-modulated-wave case, the pulse was variable from $\frac{1}{2}$ to 30 microseconds.

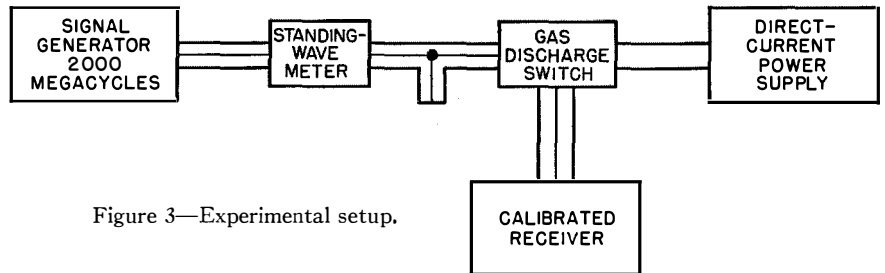


Figure 3—Experimental setup.

The pulse output could be operated synchronously with a trigger generator and could be delayed up to 300 microseconds after the trigger pulse. The transmission line was standard $\frac{7}{8}$ -inch (22-millimeter) 50-ohm coaxial line throughout. Two probes were available for the standing-wave meter. The first was a standard crystal-type probe connected to a direct-current-type galvanometer; the second was a probe that could be attached to the input of a sensitive radio receiver. The radio-frequency receiver was specially constructed for these tests. It consisted of a klystron local oscillator and a low-noise crystal mixer using a type 1N28 silicon crystal feeding a low-noise 30-megacycle intermediate-frequency amplifier.² The output of the amplifier was connected to a video-frequency terminal and a thermocouple, the latter being used for power measurements. The receiver, which had a 50-ohm input impedance, had an over-all noise factor of 11.2 decibels³ and a bandwidth

¹ Type LAG.

² A. G. Kandoian and A. M. Levine, "Experimental Ultra-High-Frequency Multiplex Broadcasting System," *Electrical Communication*, v. 26, pp. 292-304; December, 1949; see p. 299.

³ That is, the noise output referred to the input terminal was 11.2 decibels greater than the theoretical noise 7×10^{-14} watt that would be generated in the input impedance (50 ohms).

of 4.2 megacycles at a center frequency of 2000 megacycles.

Resistive attenuators, each introducing 10 decibels of loss, were used at the output terminal of the generator and the input terminal of the receiver to eliminate possible errors of measurement due to variations in the generator and receiver impedances with changes in signal level.

The power supply consisted of a direct-current variable-voltage supply, which was connected either to the gas discharge tube directly through a current-limiting resistor or to a series-type pulse modulator capable of output currents of several amperes. When pulsed power was used, a variable-pulse-width trigger generator provided for pulses from 0 to 40 microseconds in width at repetition rates from 40 to 1000 cycles.

The output terminal of the receiver was connected to a Dumont type-248 cathode-ray oscilloscope. This instrument is provided with both a free-running and servo-sweep generator and is suitable for photographing output waveforms. The servo sweep was controlled from the trigger generator for pulsed-discharge studies.

The first experiments were performed using a simple cold-cathode discharge tube. This is shown in Figure 4. The anode end is inserted in one end of the coaxial line as shown. A metallic coating covered the entire length of the tube, except for the gap *S*, and hence comprised a portion of the center conductor. The cathode was located inside the metallic coating some distance from the end of the gap, as shown, and its terminal was brought out of the coaxial line through a quarter-wavelength (at 2000 megacycles) polystyrene choke. A coaxial line to the receiver was attached to the tube a quarter wavelength from the inside end of the choke. Other tubes having similar construction could be readily inserted in place of the one shown in the figure.

The tube was connected through its tubulation to a gas-filling system so that the nature of the gas and gas pressure could be controlled readily.

The gases used in these experiments were helium, neon, argon, krypton, and mixtures of

the several gases. Nitrogen, hydrogen, and oxygen were introduced as impurities to study their effects on the rare-gas-plasma properties. The pressures ranged from $\frac{1}{2}$ to 20 millimeters of mercury. The radio-frequency power was limited to about 20 milliwatts or less in all cases.

The attenuation measurements were made with reference to a brass central conductor replacing the gas discharge tube. The radio-frequency attenuation for a given condition of the discharge was measured by raising the input radio-frequency signal level until a standard

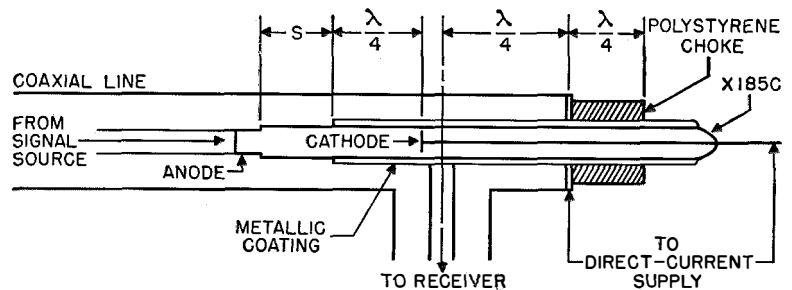


Figure 4—Cold-cathode discharge tube used in first experiments.

reading was obtained at the thermocouple output of the receiver. This method maintained the signal-to-noise ratio of the receiver constant and eliminated the possibility that nonlinear gain characteristics of the receiver might distort the measurements.

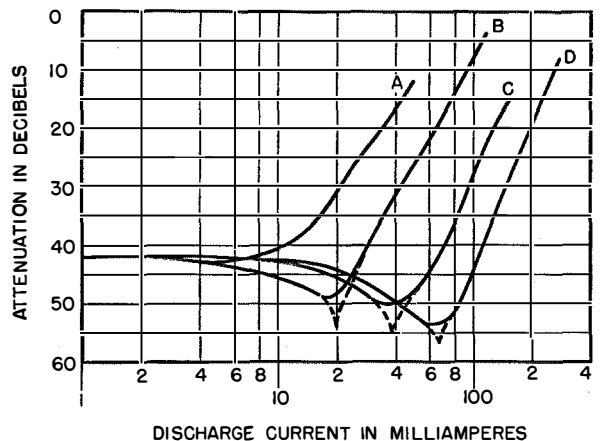


Figure 5—Attenuation as a function of discharge current for: *A*—neon with 1 percent of argon at a pressure of 4.5 millimeters of mercury and *B*, *C*, and *D*—neon at pressures of 4.5, 2, and 1 millimeter of mercury, respectively.

2. Experimental Results (Coaxial Line)

Figure 5 shows the attenuation as a function of discharge current for a neon-filled tube at several pressures, and one curve for neon with one percent of argon. Figure 6 shows the results for the same tube filled with several gases at the same pressure (2 millimeters of mercury). The

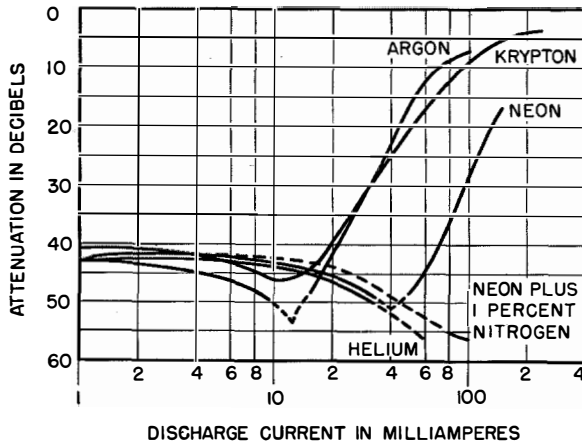


Figure 6—Attenuation as a function of discharge current for several gases at pressures of 2 millimeters of mercury.

tubes used in these experiments had an inside diameter of approximately 5 millimeters (0.197 inch) in all cases and a total plasma length of over 6 centimeters (2.36 inches). The length of the part of the plasma in the gap was approximately 2.5 centimeters (0.98 inch). It is apparent that the attenuation of the plasma is a function of discharge current for a given pressure. In particular, it is to be noted that as the current is increased, there is a sharp reduction in attenuation from a high value, corresponding approximately to the "cold" attenuation of the gap, to very low attenuation at only slightly larger currents. For example, in the case of the 4.5-millimeter curve for pure neon in Figure 5, for a current increase of from 20 to 100 milliamperes or a ratio of 1:5, the increase in power transmitted through the discharge is 42 decibels or a power ratio of $1.6 \times 10^4:1$. In addition, it is notable that for a certain low-current region, there is an increase in attenuation over that corresponding to the cold or gap attenuation. Considering the first-mentioned effect, the sharp decrease in attenuation with only a moderate increase in current is suggestive of a resonance effect.

It is evident that the plasma has attained a value of electron density that appears to be critically related to the incident signal frequency. It is known that there exists in the high-density plasma a proper frequency of oscillation that is given by the Langmuir-Tonks formula

$$\nu_p = (e^2/\pi m)^{1/2} N^{1/2}, \quad (2)$$

where

ν_p = proper frequency of plasma oscillation

e = electron charge

m = electron mass

N = electron density.

For the electronic charge, $(e^2/\pi m)^{1/2}$ has a value of 8980. The resonance observed, therefore, would appear to correspond to the value of electron density for which the plasma frequency is of the order of the signal frequency. Under these conditions, if the radio-frequency energy is not sufficiently large to cause an increase in the normal electron-collision frequency, the discharge becomes a good radio-frequency conductor at the boundary that it defines.

If the proper frequency of the plasma electrons is taken into account, the dielectric constant, in the case where the collision frequencies are very small compared to the signal frequency, is given by

$$\epsilon = 1 - \frac{\omega_p^2}{\omega_s^2 - \omega_p^2}, \quad (3)$$

where

ϵ = relative dielectric constant of plasma

$\omega_p = 2\pi \times$ proper frequency of plasma electrons

$\omega_s = 2\pi \times$ signal frequency.

Since in the cylindrical plasma there is a continuous radial distribution⁴ of electron densities having a maximum value at the axis, there is necessarily a continuous spectrum of proper frequencies ω_p limited at the high-frequency side by that corresponding to the maximum electron density. Hence, for all frequencies below this maximum frequency, critical conditions exist in the plasma. Therefore, in the case of a broad-band coaxial system, one would expect substantial radio-frequency energy transmission for

⁴ For sufficiently high electron-positive ion densities, the distribution follows the law:

$$N(r) = N_{\max} J_0 \left(\frac{2.405 r}{r_{\max}} \right).$$

all frequencies below a maximum frequency determined by the maximum electron density.

Such a geometry has an essentially wideband transmission characteristic.

An estimate of the electron density based on the random current and electron temperature⁵ at a 100-milliampere discharge current yields an electron density corresponding to a plasma frequency ω_p of 2.8×10^9 cycles per second. Hence ω_s is approximately equal to $\omega_p 2^{1/2}$. The difference between the signal frequency and the maximum plasma characteristic frequency is accounted for by the expression for ϵ .

It is to be noted that under certain pressure conditions there is a very sharp *increase* in attenuation at a current just below the rising portion of the transmission curves. Due to the already high attenuation of the gap, and instrument limitations, it was not possible to determine the nature (absorption or reflection) of this increased attenuation. In view of this limitation, no satisfactory explanation was found. It is however believed that this is an absorption phenomenon.

It is seen from Figure 5 that similar attenuation versus current curves are obtained for different pressures, and in particular that the current required for a given attenuation on the rising portion of the curve is higher for lower pressures.

This is due to two principal phenomena. First, one expects that as the pressure is reduced, the average electron velocity is increased for a given current. Accordingly a higher current is required to produce the same electron density and consequent transmission.

The second and probably greater effect is the increase in the diffusion rate of the charges to the walls at lower pressures. Since, as the pressure is reduced the rate of diffusion increases, it is apparent that the drift current necessary to obtain a given electron density is increased. Figure 7, which is a curve of attenuation as a function of pressure for krypton at a constant discharge current, illustrates this effect. The interpretation given is supported by comparisons of the attenuation in different gases at equal or nearly equal pressures. For example, from Figures 5 and 6 at 2 millimeters pressure of

⁵ Estimated density $J = Ne \left(\frac{KT_e}{2\pi m} \right)^{1/2}$
 $= 2.48 \times 10^{-14} (T_e)^{1/2} N$, amperes per square centimeter.

argon, an attenuation of 10 decibels is obtained at 70 milliamperes. For neon, the same attenuation requires 185 milliamperes. This is due to the lower diffusion rate of the heavier argon and the lower electron temperatures in that gas. A similar comparison is found between the neon, argon, and krypton gases at other pressures.

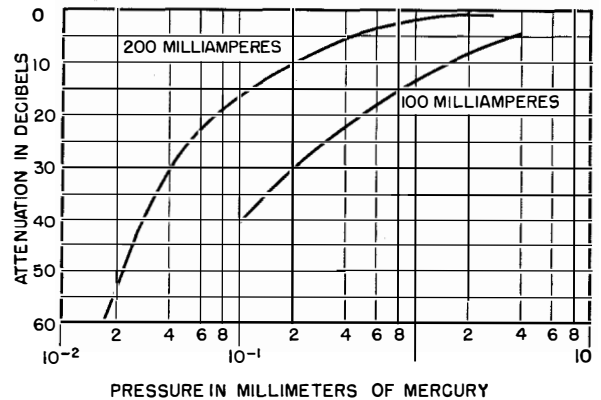


Figure 7—Attenuation plotted against gas pressure for krypton at two constant values of discharge current.

The nature of the gas has a threefold effect. First, for different gases the masses are different. Accordingly the positive-ion mobilities and hence the diffusion rate in the heavier gases are lower. Since, in the current-density region, where the diffusion is ambipolar, the electron diffusion to the walls is controlled by the mass of the positive ions, its rate will be lower in the heavier gases. In addition, the maximum electron velocities are limited by the first excitation level of the gas. Hence the maximum electron velocity will be lower in the heavier gases, which have lower excitation potentials.

So long as the amplitude of the radio-frequency signal is sufficiently small, the effect of the reduction of the first excitation level with increasing mass can be neglected from the point of view of the dissipation in the gas. This leaves then the electron temperature and the diffusion phenomena as the principal controlling factors in the electron density, and hence the imaginary conductivity for the rare gases. The experiments show that in the heavier rare gases at approximately equal pressures the same transmission is attained at lower currents. With regard to the electron removal process, if electron attachment is neglected, one finds, on comparing the possible rate of recombination with the ambipolar

diffusion rate, that the electron removal process is controlled primarily by the diffusion, in the pressure range from 1 to 10 millimeters of mercury and for the geometries used. This leads to the conclusion that the principal effect of the nature of the gas in controlling the radio-frequency transmission is the ambipolar diffusion.

3. Transmission in Molecular and Electro-negative Gases

A lower electron temperature contributes to a higher value of electron density for a given current. It has been seen from the experiments with gases that a certain minimum electron density is required for good transmission (i.e. the insertion loss must be small compared to the "cold" insertion loss) in a geometry of this type. This concept may be expanded to include other geometries in the sense that the critical value of ϵ in such other geometries represents the region

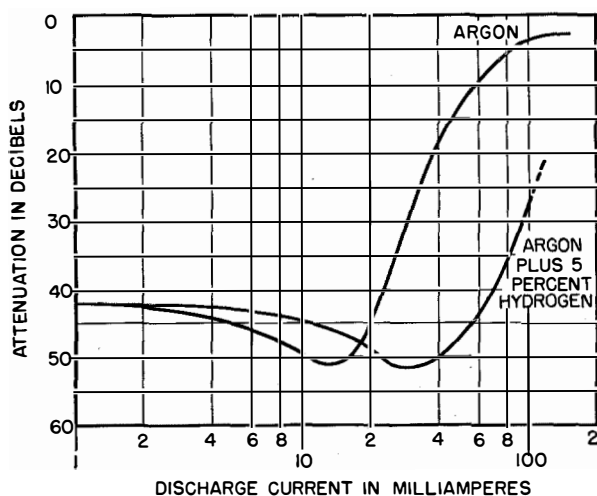


Figure 8—Effect on attenuation of adding 5 percent of hydrogen to argon at a pressure of 1.5 millimeters of mercury.

of low radio-frequency-field penetration. Accordingly, it may be deduced that the imaginary conductivity is high under these conditions. It is obvious that for an imaginary conductivity σ_i large compared to the real part of the complex conductivity σ_r , the mean free time T_f of the electrons must be large compared to $1/\omega_s$. For if $\omega_s \sim 1/T_f$, a large fraction of the radio-frequency energy that has been transferred to the electrons is transferred by the electrons to the atoms of the gas and hence lost. If $\omega_s \ll 1/T_f$,

relatively little energy can be transferred to the electrons and little or no propagation can take place in the mode considered.

In the case of a molecular gas of a nonelectro-negative nature, such as hydrogen or nitrogen, there are molecular vibrational and rotational excitation levels possible. Therefore, if we consider the probability of cumulative ionization larger than direct ionization, a very large number of electrons is necessary merely to maintain ionization, and hence a large current is required to obtain a given net electron density for the support of a radio-frequency wave.

One would expect, therefore, that to attain a sufficiently high density of electrons having a sufficiently long mean free time to contribute to the propagation of the radio-frequency signal, a very much higher current would be required, as compared with the rare gases. In the case of a mixture of a molecular gas such as hydrogen with a rare gas such as argon, even a small percentage of hydrogen molecules will contribute to the loss of electron density and hence raise the current required. In addition, the principal ionization is in the hydrogen, which has a very much lower mass than argon. Hence, one would expect the ambipolar diffusion rate to be much greater than in pure argon. This tends to decrease further the electron density for a given current density.

The over-all effect is to reduce the radio-frequency transmission; that is to increase σ_r at the expense of σ_i . This is demonstrated in Figure 8, which shows the effect of 5 percent of hydrogen in argon at 1.5 millimeters of mercury. From the curves, for pure argon an attenuation of 30 decibels is obtained at 32 milliamperes, while the same attenuation is obtained in the mixture at 92 milliamperes.

Figure 9 illustrates the effect of the molecular gas without the increased rate of diffusion provided by the hydrogen. In this case, the mixture of 6 percent of nitrogen in helium is compared with helium alone at 4 millimeters pressure, and similar results to the former case are obtained.

In the case of electronegative gases such as oxygen, chlorine, etc., a situation similar to the nonelectronegative molecular gases exists. In these gases, the low-velocity electrons are attached in collision with the gas molecules forming

negative ions. Since the mass of negative ions is large, they cannot contribute to the high radio-frequency transmission. Hence the effect of the negative ions formed in the presence of an electro-negative gas is to reduce the electron density for a given current. This results in a very much higher current requirement for a given radio-frequency transmission.

The method, described here, of examining the radio-frequency transmission of a gas discharge plasma in a coaxial geometry is suitable to determine concentrations of metastable atoms in the rare-gas discharges. This method compares the electron densities with the radio-frequency transmission characteristic in the gas to be investigated and with the same gas at the same pressure mixed with a small but adequate percentage of a quenching gas. This effect is obtained for example in neon ($V_{met} = 16.6$ electron volts) by mixing a small percentage of argon ($V_{ion} = 15.7$ electron volts) with the neon gas. In this case, a higher radio-frequency transmission occurs and hence higher electron density at lower current. This is shown by comparison of 4.5-millimeter curves for neon and for neon plus 1 percent of argon in Figure 5.

4. Phase-Shift Measurements of Wave Propagation in a Plasma-Filled Waveguide

It is well known that the phase velocity of a wave propagated in a dielectric medium is a function of the dielectric constant of that medium. The dielectric here considered is a free electron gas supported by a gas discharge plasma.

Experiments were performed in a rectangular waveguide substantially filled with a gas discharge plasma. The results below are relative to a signal frequency of 9450 megacycles. The gas discharge plasma was contained in a rectangular glass envelope, the walls of which were immediately adjacent to the metallic waveguide surface. The electrodes for the maintenance of the direct-current plasma were arranged so as not to interfere with the transmission of the high-frequency waves through the guide.

The wavelength of a wave propagating in a rectangular waveguide is given by

$$\lambda_g = \frac{\lambda}{\left[1 - \left(\frac{\lambda}{\lambda_c}\right)^2\right]^{\frac{1}{2}}} \quad (4)$$

for an evacuated waveguide ($\epsilon_0 = 1$). In the case of a waveguide filled with a dielectric constituted by a gas discharge plasma, the guide wavelength is given by

$$\lambda_g = \frac{\lambda}{\left[1 - \left(\frac{\lambda}{\lambda_c}\right)^2 \left(\frac{1}{1 - \frac{4\pi N e^2}{m\omega^2}}\right)\right]^{\frac{1}{2}}} \quad (5)$$

(when the imaginary part of the dielectric coefficient is negligible compared to its real part).

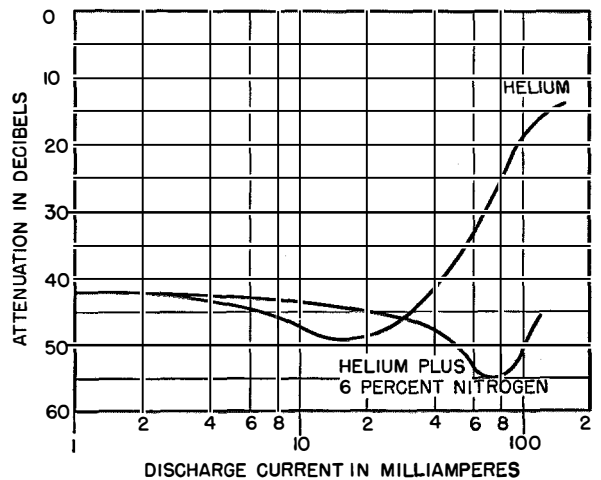


Figure 9—Effect on attenuation of adding 6 percent of nitrogen to helium at 4 millimeters pressure.

N is the electron density, assumed here to be uniform over the cross section of the guide.

The variation in λ_g due to the dielectric constant of the plasma results in a phase shift of

$$\phi = \frac{2\pi}{\lambda} \left\{ \left[1 - \left(\frac{\lambda}{\lambda_c}\right)^2 \right]^{\frac{1}{2}} - \left[1 - \left(\frac{\lambda}{\lambda_c}\right)^2 \left(\frac{1}{1 - \frac{4\pi N e^2}{m\omega^2}}\right) \right]^{\frac{1}{2}} \right\} \quad (6)$$

radians per unit length. It is then expected that one could produce a variation in λ_g by varying the electron density N . This of course is readily accomplished by controlling the discharge current.

The experiments were performed using a waveguide section 45 centimeters long. A bridge arrangement, shown in Figure 10, was used for the determination of the phase shift. With no

discharge present, the position of the standing-wave minimum was determined and the shift in position measured as a function of discharge current.

ductivity tests. A galvanometer, connected to the thermocouple, was used to indicate the radio-frequency power into the receiver.

The most convenient power standard available (for a large number of successive measurements) was the receiver noise itself. Accordingly, all noise measurements were made with reference to the receiver noise. Periodic checking of the receiver noise factor against a standard-signal generator insured the accuracy of this reference.

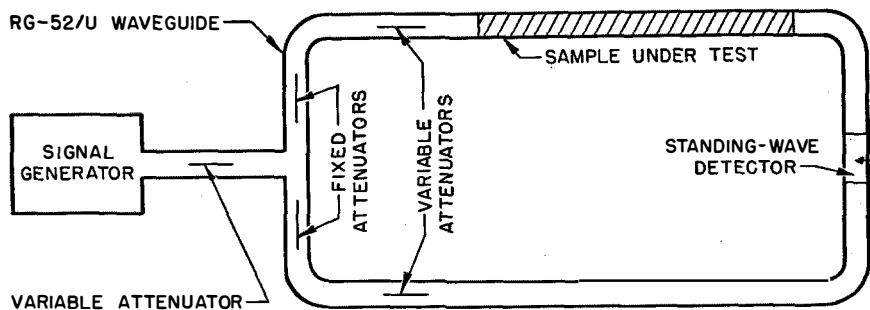


Figure 10—Test setup for measuring phase shift through a gas-discharge-plasma-loaded waveguide.

Figure 11 shows the phase shift as a function of discharge current. It will be noted that, under the particular conditions indicated, the phase shift is a substantially linear function of current. This type of measurement leads to a convenient method for determining average electron densities.

The noise measurements were made in a limited bandwidth, and it is to be remembered that the values obtained are power averages over the band. In view of the high frequency used (2000 megacycles), this does not represent a serious limitation on the quality of the measurements.

5. Presence of Noise in Gas Discharge Plasma

It has become evident that the electrons in the gas discharge plasma are capable of supporting radio-frequency signals incident upon it. That is, the plasma is a medium in which wave propagation obtains due to the interaction fields among its constituents. One would expect, therefore, that under favorable conditions (i.e. negligible absorption) and in favorable geometries, any local disturbance within the plasma would be propagated through it and produce an observable effect in an external circuit. One would expect this effect to be of the nature of random noise.

To study the existence and nature of this noise, an experimental setup was arranged as follows.

The same type of microwave setup used in the transmission measurements was used for noise measurements. It is shown in Figure 12. The load was a 50-ohm coaxial load that matched the transmission line. The other microwave terminal pair was connected to the receiver through a short coaxial cable.

The receiver was the same used for the con-

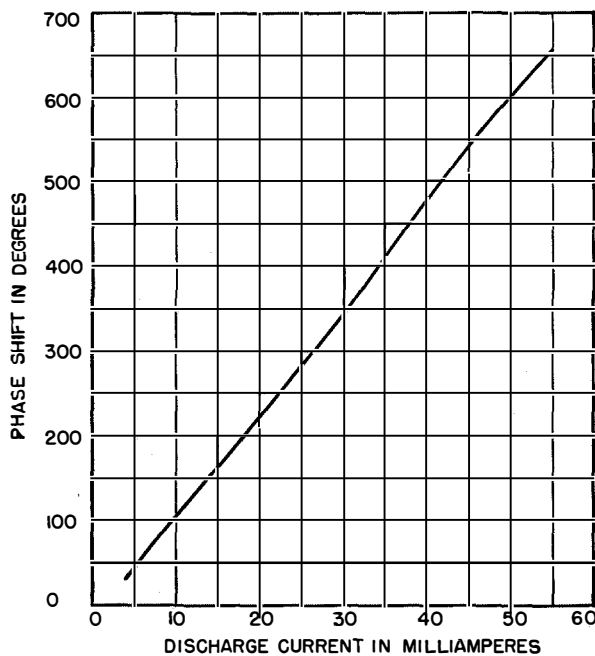


Figure 11—Phase shift plotted against discharge current for 18 inches (46 centimeters) of RG-52/U waveguide within which was a rectangular glass tube 1.9 by 0.8 centimeters (0.75 by 0.315 inch) filled with neon and argon at a pressure of 1.5 millimeters of mercury. The excitation frequency was 9450 megacycles.

6. Noise Experiments and Experimental Results

A considerable number of noise measurements as a function of the nature of the gas, gas pressure, and the discharge current were made for a direct-current discharge. In general, the results were similar to those presented here, and these

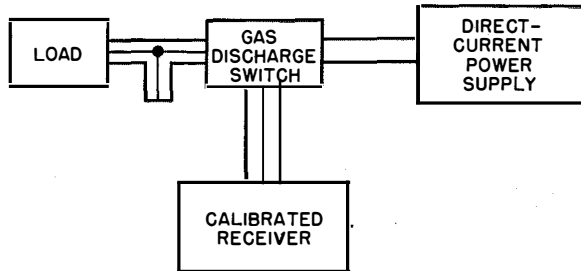


Figure 12—Equipment arrangement for noise measurement.

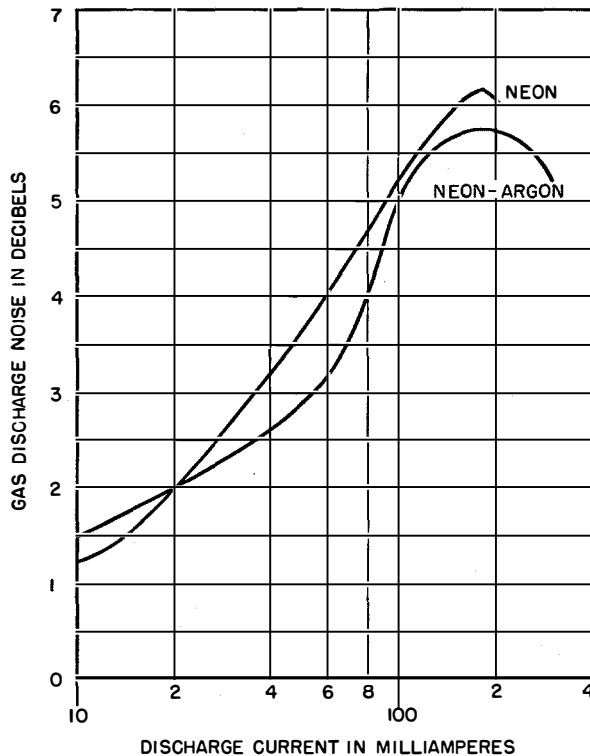


Figure 13—Plotted against discharge current in milliamperes is the gas discharge noise in decibels referred to a level corresponding to the receiver output noise, which was 11.2 decibels above the theoretical noise of 7×10^{-14} watt for a bandwidth of 4.2 megacycles at 2000 megacycles. The curves are for neon at 1 millimeter pressure and for neon plus 1 percent of argon at 2 millimeters pressure.

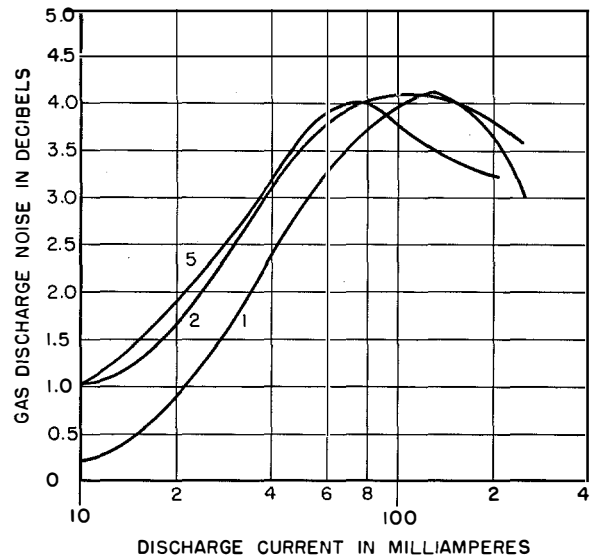


Figure 14—Curves similar to those of Figure 13 but for krypton at the indicated pressure in millimeters of mercury.

are typical. The particular measurements made were for continuous direct-current discharge conditions in a hot-cathode tube. The cathode was shielded by a tantalum cylinder, which is entirely outside the radio-frequency circuit. A sketch of the tube is shown in Figure 1.

The noise observations were made in the absence of any radio-frequency signal.⁶ Typical experimental curves available are shown in Figures 13, 14, and 15. It is seen that they all have similar characteristics, rising to a broad smooth peak in the 60-to-150-milliamperere range and then decreasing, for all gases and pressures used. Equipment limitations prevented measurements for currents greater than about 250 milliamperes in most cases. Figure 16 shows the attenuation and the corresponding noise

⁶ In the presence of an externally applied radio-frequency signal of considerable amplitude, it was observed experimentally that an oscillation in the region from 5 to 20 kilocycles per second appeared. The amplitude of this oscillation increased with increasing signal amplitude. This oscillation can be accounted for only by the discharge tube itself, and evidently appears in the output of the 2000-megacycle receiver due to a modulation by the discharge plasma of the radio-frequency signal by a low-frequency oscillation generated within the plasma. This oscillation frequency is too low to be accounted for by either an ionic collisional noise or a plasma oscillation. It is probable that the low-frequency signal is due to a hydrodynamic type of oscillation. Since this low-frequency oscillation is apparently capable of modulating an externally applied signal, it is probable that it also modulates the high-frequency noise produced in the discharge, increasing the total noise energy radiated by the discharge.

characteristic as a function of current for krypton at a pressure of 2.3 millimeters. It is apparent that the peak of the noise characteristic occurs in the current region of the knee at the top of the transmission characteristic.

In view of the limited experimental information available in 1946–1947, when this work was conducted, it was difficult to draw any definite conclusions as to the cause and nature of the

noise generated in the discharge plasma, but it now seems likely that the noise at high frequencies is due to collisional noise, electronic density fluctuations in the plasma, or more probably both.⁷⁻⁹

7. Experimental Study of Radio-Frequency Transmission Under Transient Conditions

Since experimental facilities (as well as power dissipation within the discharge) limited the use of direct-current in excess of 250 to 300 milliamperes, it was found desirable to apply pulse techniques to obtain higher discharge currents and hence higher electron densities. Thus, while in the direct-current discharge, transmission never reached 0 decibel, it appeared possible to determine whether an increase in transmission occurred at higher electron densities not otherwise attainable. By the application of a short pulse of the order of a few microseconds of high amplitude, the entire transmission characteristic, for a wide range of electron densities in the disintegrating plasma, is readily observable. By the same token, disintegration times of the decaying plasma, and the law of disintegration can be obtained.

By using a radio-frequency signal essentially as a probe to study the discharge plasma the limitations imposed by the permanent nature of the usual physical probe are avoided. The radio-frequency signal probe may be applied or removed at will and, furthermore, its time of application and removal relative to the initiation of the discharge may be controlled over limits determined only by the complexity of the auxiliary apparatus used. Because the radio-frequency field will be used as probe, its amplitude must be sufficiently small so that the energy contributed by it does not materially affect the normal electron energy distribution within the discharge. Specifically, the amplitude of the radio-frequency field must be such that

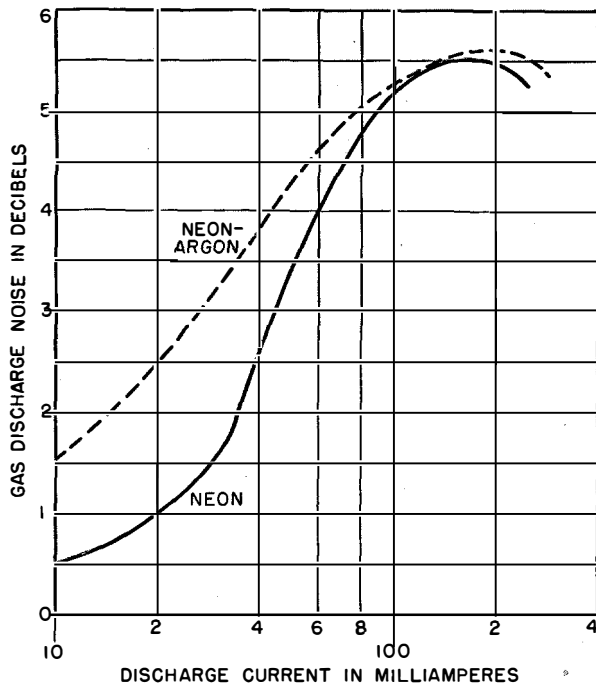


Figure 15—Curves similar to those of Figure 13 but for neon and neon plus 1 percent of argon at pressures of 5 millimeters of mercury.

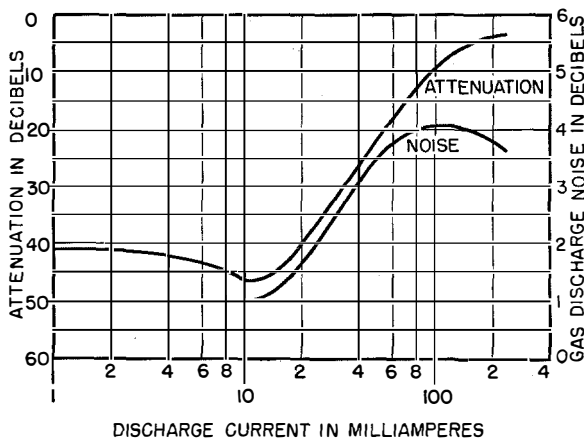


Figure 16—Attenuation and noise plotted against discharge current for krypton at a pressure of 2.3 millimeters.

⁷ L. Goldstein and N. L. Cohen, "Radiofrequency Conductivity of Gas-Discharge Plasma in the Microwave Region," *Physical Review*, v. 73, p. 83; January 1, 1948.

⁸ W. W. Mumford, "Broad-Band Microwave Noise Source," *Bell System Technical Journal*, v. 28, pp. 608–618; October, 1949.

⁹ P. Parzen and L. Goldstein, "Current Fluctuations in the Direct-Current Gas Discharge Plasma," *Physical Review*, v. 82, pp. 724–726; June 1, 1951.

the amplitude of electronic oscillations imposed by the field are very much smaller than the normal electronic mean free path.

By varying the frequency of the radio-frequency signal, phenomena that differ with gas pressures may readily be examined.

It is to be noted that this method of studying the discharge is limited to those processes that involve the electron density and electron distribution functions of the discharge. In addition, the sensitivity of the method depends principally on the noise generated by the receiver.

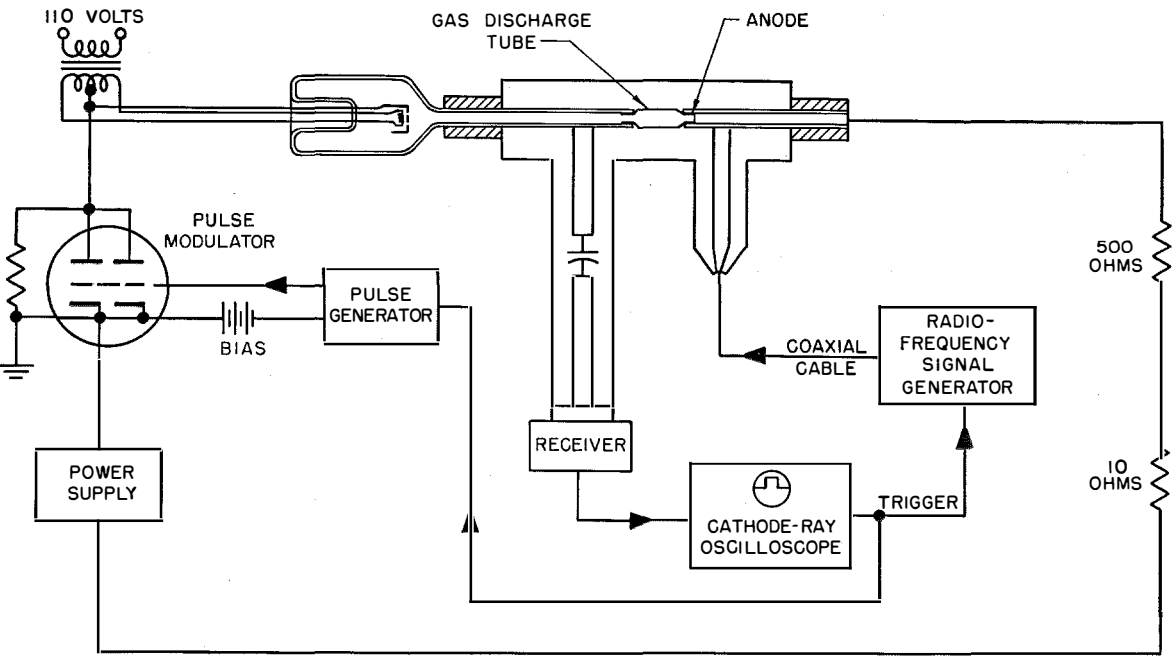


Figure 17—Pulse-transmission setup.

The decay or disintegration of the plasma after removal of the exciting field is a fruitful region for study by this method.¹⁰ The disintegration time observable by means of the radio-frequency signal, of course, depends on the nature of the gas, gas pressure, and intensity of the discharge. The times of decay of transmission (and, hence, electron densities) observable by this method at the frequency used exceeded several microseconds, in even the most mobile gases at pressures of the order of 1 to 10 millimeters of mercury. In addition, it is possible to examine in some detail production of electrons by secondary sources during the disintegration time. The time limitation in this case is the disintegration of the electron density to a level that results in a radio-frequency signal attenuation down to the receiver noise level.

¹⁰ Since this work was started, a similar method has been described by S. C. Brown *et al.*, Massachusetts Institute of Technology, Research Laboratory of Electronics Report; May, 1948.

The method is obviously only sensitive to variations in electron density that cause a change in the radio-frequency signal output at least as great and preferably greater than the amplitude of the receiver noise.

The types of measurements that are possible with the radio-frequency equipment are essentially of two kinds. The first of these is the power transfer measurement, and the second is the power reflection measurement. These may be likened to measurement of the iterative and transfer impedances of a two-terminal pair.

In the most practical terms, the first measurement is an attenuation measurement of the amount of radio-frequency signal that appears at the output of the gas discharge for a given input. The second measurement is the voltage-standing-wave-ratio measurement common to distributed-parameter experimental work.

8. Experimental Setup and Method of Measurement for Transient Transmission

The experimental setup for the transient transmission measurements is shown in Figure 17.

The gas discharge tube was placed in the coaxial line as in the case for the direct-current measurements. The anode was connected through a current-limiting resistor to the direct-current power supply. The cathode of the discharge tube was connected through a "series" pulse modulator to ground. The pulse modulator was shunted by a relatively high resistance that allows a small current to be maintained in the discharge tube, as desired. The pulse modulator consisted of two type 3E29 tubes in parallel operating in the normally cut-off condition. The grids of the modulator tubes were supplied by a pulse from a pulse generator. The amplitude of the pulse was adjustable, as was the duration. The pulse duration was from $\frac{1}{2}$ to 100 microseconds. For pulse durations up to 10 microseconds, the rise time was approximately $\frac{1}{4}$ microsecond with a flat top and a decay of about $\frac{1}{4}$ microsecond. For pulse durations exceeding 10 microseconds, the pulse had a rise time of about 1 microsecond.

The radio-frequency signal generator was connected to one of the radio-frequency terminals. The same receiver used in the direct-current discharge transmission and noise measurements was connected to the other output terminal of the coaxial line, through a 20-decibel radio-frequency attenuator section. The output of the receiver was connected to a Dumont type-248 cathode-ray oscilloscope. This oscilloscope is provided with a servo sweep of adjustable duration and time markers for calibrating the sweep. It also contains a trigger-signal generator, which was used to trigger the pulse generator and servo sweep simultaneously. The radio-frequency signal generator could be operated either with a continuous-wave signal output or with a pulsed radio-frequency signal output. The radio-frequency pulse was adjustable over a range of $\frac{1}{2}$ to 30 microseconds, and could be delayed from the trigger time up to 300 microseconds. The trigger source in the cathode-ray oscilloscope was used to trigger the radio-frequency pulse, when required.

With this arrangement, it was possible to examine the radio-frequency transmission as a function of time in two ways.

The first method was to scan the transmission pulse arising out of the applied discharge pulse with a narrow radio-frequency pulse. With this method, the radio-frequency pulse was set at any desired time up to 300 microseconds after the discharge-current pulse, and the attenuator on the signal generator was set for a standard amplitude of the detected radio-frequency pulse on the cathode-ray tube. The reference level used was the transmission with the discharge tube off. This method allowed detailed examination of the transmission phenomena, and in principle appeared useful. It was found, however, that in certain cases for various reasons the radio-frequency transmission of the decaying plasma

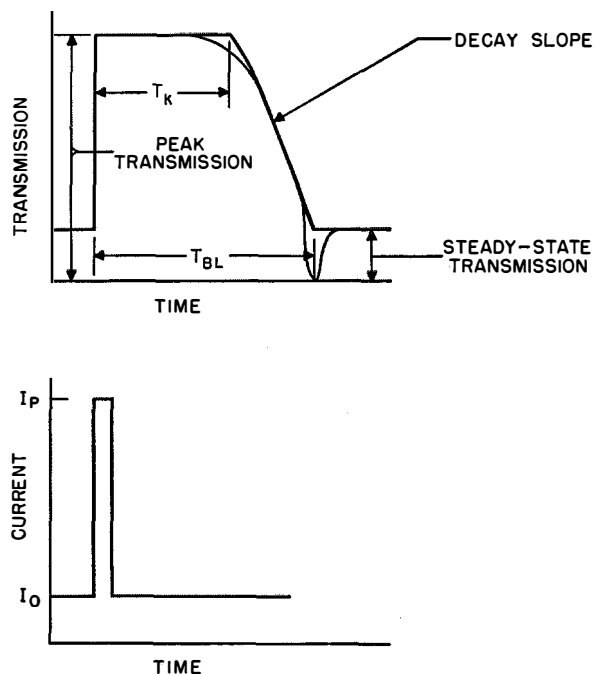


Figure 18—Idealized forms of transmission and excitation pulses.

changed slowly with time. Since this method of study required considerable time for accurate measurements, a second semi-quantitative method was also used.

This involved applying a continuous-wave radio-frequency signal to the discharge tube and photographing the cathode-ray tube while the discharge was being pulsed. This necessitated

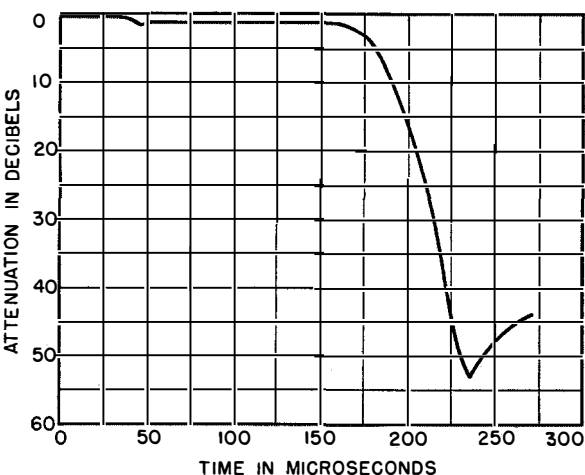


Figure 19—Attenuation values immediately following the removal of a discharge pulse in argon at a pressure of 1.5 millimeters of mercury. The pulse went from a steady-state current of 25 milliamperes to a peak value of 1.5 amperes for 10 microseconds. The ranges of uncertainties for the curve are 20 microseconds and 2 decibels.

operating the discharge for only a few seconds at a time. The results obtained were of limited utility, since the measurements had to be made from a photograph of the transmission pulse. In addition, it was desirable to place considerable attenuation between the radio-frequency output of the coaxial line and the receiver input. This limited the dynamic range observable to about 20 decibels above the receiver noise level in most cases. It did allow an accurate determination of the flat portion of the transmission and the upper part of the decay characteristic, in keeping with the repeatability of the experiments, and in this respect was very useful. The general transmission pulse shape is shown in Figure 18.

9. Experiments and Results

The first experiments were performed using the pulse-scanning method. The results indicated that, in general, the attenuation characteristic of a disintegrating plasma in a rare gas are described essentially by a curve with a flat portion of relatively low attenuation for some time after the removal of the driving pulse, a rapidly increasing attenuation to a value greater than the steady-state condition, followed by a return to the normal steady-state value.

A typical attenuation characteristic is shown in Figure 19. This particular measurement was

made under the conditions indicated. It is to be noted that, in this case, the attenuation of the gap is only slightly larger than 0 decibel for about 40 microseconds after the removal of the energizing pulse. Thence there is a drop to a slightly larger attenuation until about 170 microseconds, when a rapid change sets in. It is to be noted that the maximum attenuation exceeds the "ultimate attenuation" determined by the value of the keep-alive current. This particular curve is more or less typical of the type of attenuation characteristic found with rare gases. The small variation in the transmission at around 40 microseconds appears to be due to a phenomenon that acts to alter suddenly the electron density or energy-distribution function, and is of the order of magnitude of the minimum variation to which the radio-frequency method is sensitive.

It is now of interest to examine in some detail the observed properties of the disintegrating plasma.

The cases discussed below were all studied in a hot-cathode gas discharge tube. Several different tubes were used, but all had essentially the same structure in the region of the gap. This construction is shown in Figure 1.

The several experiments performed were made in hydrogen, the rare gases, and mixtures of the

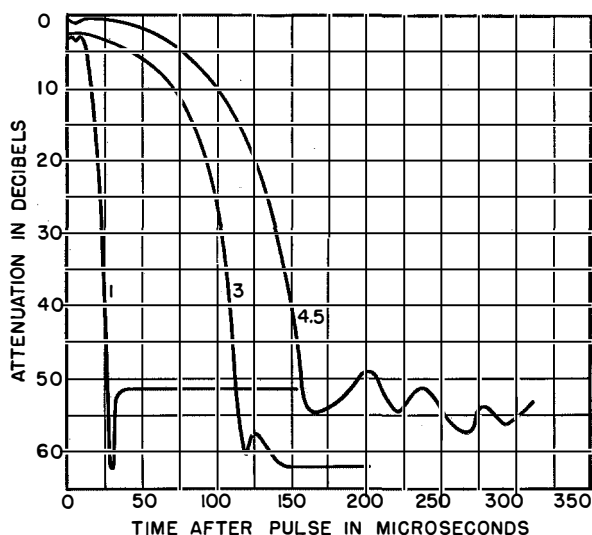


Figure 20—Attenuation plotted against time after the discharge pulse for helium at the indicated pressures in millimeters of mercury. The discharge pulse went from a steady-state current of 30 milliamperes to a peak value of 0.5 amperes.

rare gases at pressures up to about 10 millimeters of mercury. The controllable variables in the experiments were the duration of the exciting pulse, pulse amplitude, pressure, and nature of the gas.

Figure 20 shows the attenuation of the disintegrating plasma as a function of time for

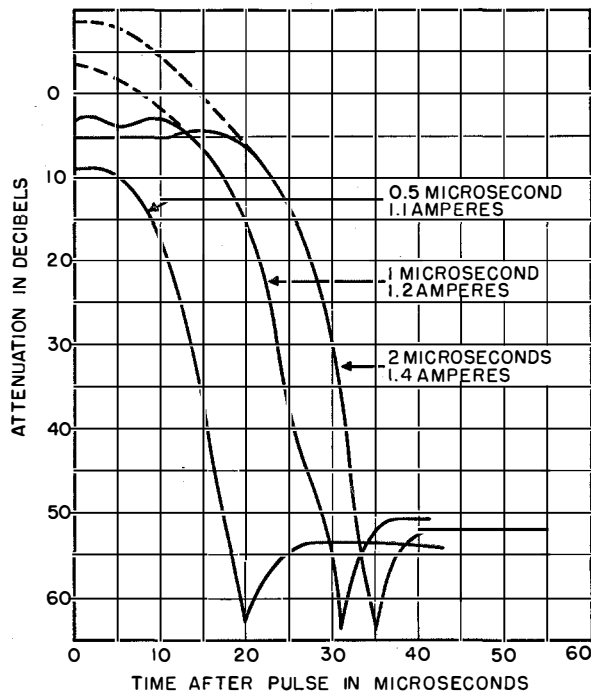


Figure 21—Attenuation after discharge pulses for helium at 1 millimeter pressure for pulses of the duration and current amplitudes indicated on the curves. The steady-state current was 30 milliamperes in each case.

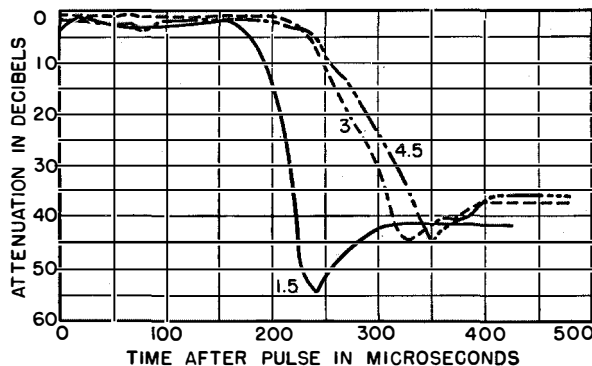


Figure 22—Attenuation plotted against time after a 1-microsecond discharge pulse in argon at the pressures indicated in millimeters of mercury. The pulse current was 1 ampere and the steady-state current was 25 milliamperes.

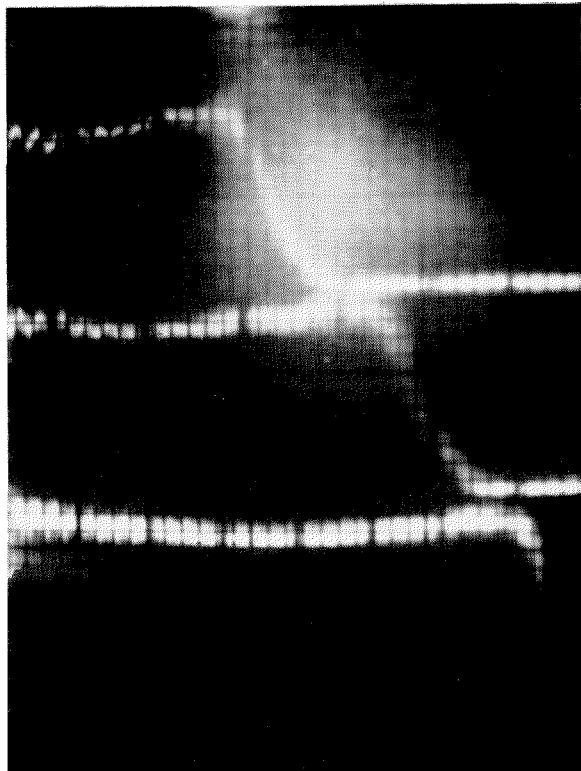


Figure 23—Oscillograms of transmission properties of neon with 1 percent of argon at pressures of 1 (uppermost curve), 2, and 3 millimeters of mercury. Steady-state current was 25 milliamperes with 1.5-ampere 1-microsecond pulses. The markers are at 10-microsecond intervals.

helium at 1, 3, and 4.5 millimeters pressure, other conditions being the same. It is seen that the duration of the transmission pulse increases with pressure. Figure 21 shows attenuation for helium at 1 millimeter pressure for exciting pulses of 0.5, 1, and 2 microseconds in duration. Here, it is seen that the duration of the transmission pulse is a function of the duration of the exciting pulse. Figure 22 shows the characteristics for argon at three different pressures. Here, again, the transmission time increases with pressure. Figures 23, 24, and 25 show transmission of the disintegrating plasma for various experimental conditions. It will again be noted that the general shape of the transmission pulse is similar to the pulse shown in Figure 18. T_{BL} (Figure 18) is taken as an arbitrary reference corresponding to the point where the received radio-frequency signal is of the same order as the receiver noise (i.e. 20 decibels below the maximum received-signal value). From some of these

data, Figures 26 and 27 have been prepared. From Figure 26, it appears that the duration of the transmission increases approximately linearly with the amplitude of the exciting pulse, as would be expected. Other conditions being constant, the total number of electrons produced is proportional to the current, and if those phenomena that act to remove the electrons are essentially linear, it would be expected that the total transmission decay time would increase with increasing initial supply, up to the point where the electron-removal processes operate at rates comparable with the production process. From this set of curves, it also is apparent that the total decay time increases with the larger gas mass, with the exception of neon-argon mixture. This case is somewhat different and will be discussed later.

Figure 27 is a plot of transmission decay slope (i.e. from the end of the "flat portion" to the base line), as a function of exciting pulse current, other conditions being constant. Here it is evident that the rate of decay is lower in the heavier gases, again with the exception of the neon-argon mixture. All of these curves show a sharp peak in slope below about 0.8 ampere. Disregarding this for the moment, it would appear that both the total decay time and the decay time beyond the flat portion of the transmission characteristic increases with increasing mass. Now the principal causes of disintegration of the electron density in the plasma are due to three possible phenomena. They are diffusion, recombination, and attachment.

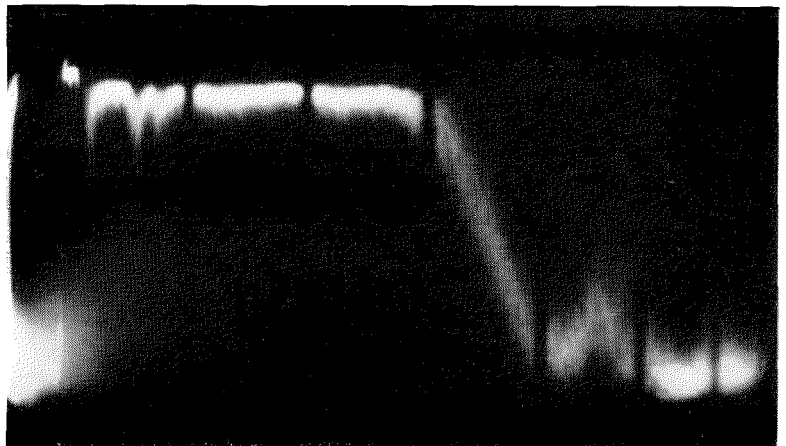
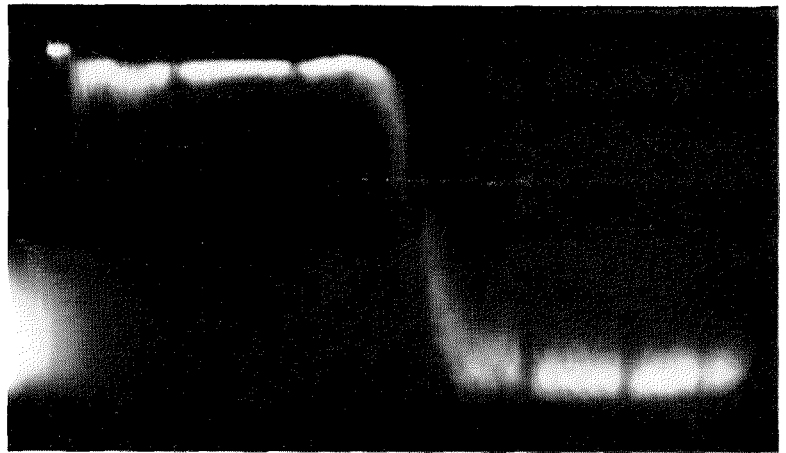


Figure 24—These two oscillograms are for neon at 1 millimeter of pressure following 1-microsecond 1.5-ampere pulses. Upper curve is for a steady-state current of 25 milliamperes while the lower curve is for zero steady-state current. The markers are at 10-microsecond intervals.

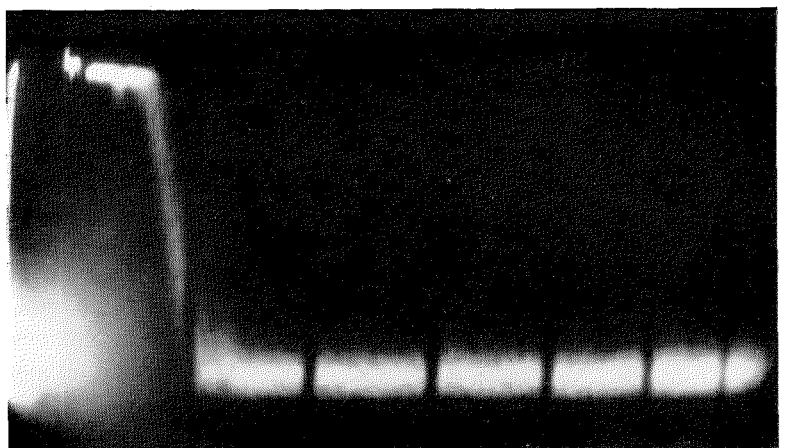


Figure 25—Behavior of argon at 1 millimeter pressure following 1-microsecond 1.5-ampere pulse from zero steady-state current. Markers are at 10-microsecond intervals.

The gases used, according to the manufacturer, contained no measurable amount of electronegative gases. The possibility of oxygen, the principal electronegative impurity likely to be present, was determined essentially by the exhausting and gas-filling system. Hence, if any electronegative impurity existed, it probably existed in about the same proportion in all gases. It may be noted that the usual precautions were made to minimize the possibility of impurities being present in the gas. This leaves then the possibility of recombination and diffusion. Since the recombination coefficients in the rare gases are of the same order of magnitude and in general quite small (although for thermal electrons fairly large),¹¹ it would appear that

¹¹ M. A. Biondi and S. C. Brown, "Measurements of Ambipolar Diffusion in Helium," *Physical Review*, v. 75, pp. 1700-1705; June 1, 1949.

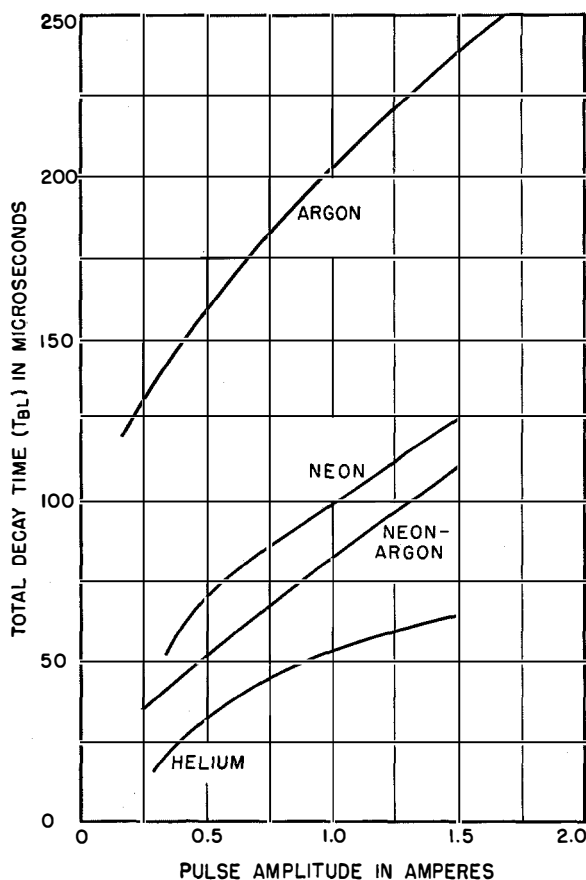


Figure 26—Total transmission decay time T_{BL} plotted against the amplitude of a 1-microsecond pulse, starting from a 20-milliampere steady-state condition, for several gases at pressures of 2 millimeters of mercury. Neon-argon indicates 1 percent of argon in neon.

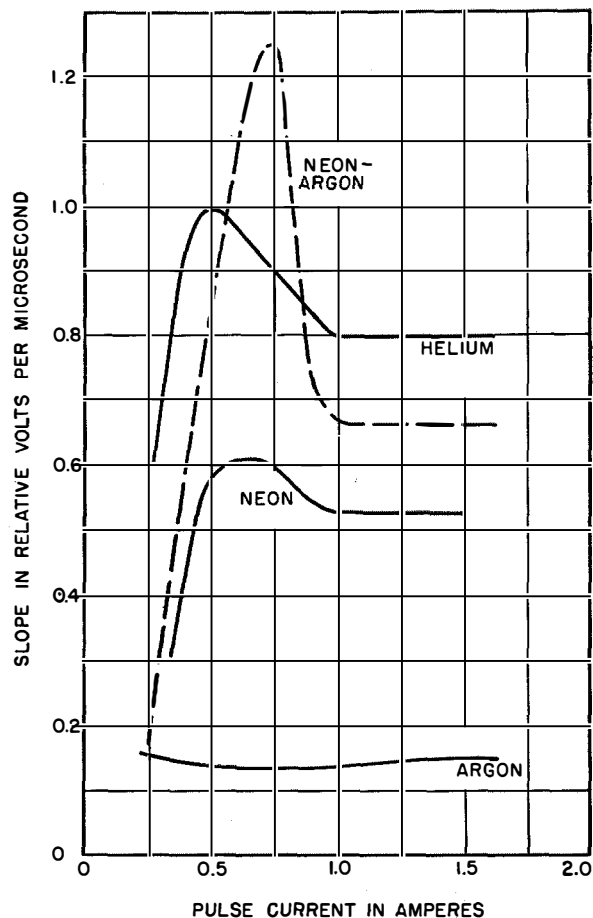


Figure 27—Rate of transmission decay as a function of the amplitude of 1-microsecond pulses starting from 20 milliampere steady-state conditions. The gases indicated (neon-argon being 1-percent argon) are at pressures of 2 millimeters of mercury.

at these pressures and in this geometry the principal cause of electron removal is the diffusion phenomenon.

Comparing the curves of neon with neon plus 1 percent argon in Figure 27, it appears that in the presence of a quenching gas, the mass of the gas is not the principal factor in determining the duration of the disintegrating plasma. It is noted that the rate of decay of the neon-argon mixture is considerably greater than that of pure neon, which evidently has approximately the same mass. It would appear that the retransfer of accumulated potential energy of the excited atoms into kinetic energy of secondary electrons is an important factor in the duration of the disintegrating plasma. The rapid quenching

action of the argon atoms on the neon metastable states removes them as a source of potential energy for the production of secondary electrons in the disintegrating plasma, thereby shortening the life of the plasma.

Furthermore, in the disintegrating plasma, since in the mixture the ions are mainly argon ions, the ambipolar diffusion rate is greater than the diffusion rate of neon ions in neon, or argon ions in argon. This is due to the improbability of charge exchange between the argon ions and neutral neon atoms. This would seem to be confirmed by the position of the neon-argon curve in Figure 27.

In the pressure range investigated (1 to 10 millimeters of mercury), and for electron densities high enough that the main removal process is diffusion (in these cases ambipolar), one expects a longer disintegration time with increasing pressure. An example of the experimental data in this connection is shown in Figure 20.

10. Conclusion

It is well known that an electron gas can define boundaries for the propagation of an electromagnetic wave. Ionospheric studies have determined that relatively low free-electron densities (approximately 10^6) provide conductive boundaries at low radio frequencies but a refractive medium to wave propagation at higher radio frequencies.

An experimental study of this phenomenon has been made in the microwave region in a waveguide system, the necessary high electron densities associated with these frequencies being obtained by the use of space-charge compensation. This necessary space-charge compensation is most readily obtained by use of the positive ions existing in the gas discharge plasma.

The experiments show that the high electron densities required for propagation in this region with no appreciable losses are readily obtained with the use of limited exciting power.

In the course of this work, it became apparent that the techniques developed are applicable to the study of many of the detail phenomena occurring in gas discharges.

Correction for

Suppression of Harmonics in Radio Transmitters

By GEORGE T. ROYDEN

IN this paper, which appeared on pages 112 through 120 of Volume 28, Number 2, dated June, 1951, equation (4) on page 117 should be

$$C = \frac{A}{(r + rR^2/F^2)^{\frac{1}{2}}}$$

Magneto-Optics of an Electron Gas for Guided Microwaves: Propagation in Rectangular Waveguide*

BY LADISLAS GOLDSTEIN, M. A. LAMPERT, AND J. F. HENEY

Federal Telecommunication Laboratories, Incorporated; Nutley, New Jersey

WE have previously described¹ magneto-optical effects in microwave propagation experiments in circular waveguide. The magneto-electronic medium in the guide was an electron gas immersed in a uniform direct-current magnetic field parallel to the axis of the guide. The main experimental results consisted of polarization transformations of a TE_{11} wave initially launched in the guide with linear polarization. The results were interpreted satisfactorily in terms of the different propagation characteristics in the anisotropic medium of the two oppositely rotating, circularly polarized TE_{11} modes that the empty circular guide supports.

The purpose of this note is to describe the results of propagation experiments with the same magneto-electronic medium in a rectangular waveguide. Both the results and their interpretation are quite different from those briefly mentioned above. In this case, the empty guide at the frequency employed supports only one propagating mode, namely the TE_{10} mode so that no polarization transformations can take place. The relevant propagation measurements in the empty guide outside of the medium are those of the amplitudes and phases of the transmitted and reflected waves. The main results of these measurements are—A) very large attenuations of the signal in the region of magnetic-field intensities where the gyrofrequency of the electrons approximates the signal frequency; B) large reflections at magnetic-field intensities immediately on either side of gyroresonance; and C) small or negligible reflection at gyroresonance. Thus, the very large attenuation at gyroresonance appears to be the result of absorption in the medium in accordance with theoretical prediction. In the accompanying figure, these results are illustrated for a particular experiment under conditions there indicated.

Further results are—A) increasing the gas pressure tends to widen the resonance and decrease its magnitude; B) at sufficiently low pressure (below about 0.1 millimeter of mercury in our experiments) the width of resonance appears to be determined by other factors than pressure, such as nonuniformity of magnetic field in the medium; and C) the phase of the reflected wave varies very sharply in the gyroresonance region. That these results are essentially independent of the gas is evidenced by the fact that similar phenomena were observed also in krypton, xenon, hydrogen, and mercury vapor.

The resonance curves have precisely the shape to be expected from the typical anomalous dispersion of the dielectric constant in the region of a proper frequency of the medium, here the electron gyrofrequency. The anom-

alous dispersion of the magneto-electronic medium has been previously established² at lower frequencies. However, in our experiments the length of the anisotropic medium exceeded two free-space wavelengths; so that true propagation phenomena have been observed.

We believe that the observed phenomena are general, to the extent that they are characteristic of electromagnetic wave propagation in the magneto-electronic medium (with longitudinal magnetic field) in any guiding system that supports only a single mode of propagation at the frequency employed.

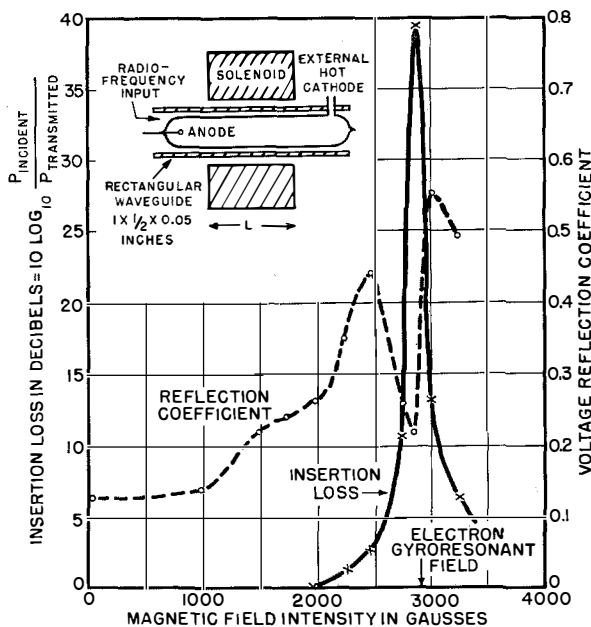


Figure 1—Transmission and reflection characteristics versus magnetic field intensity. Signal frequency = 8200 megacycles per second. Gas is neon plus 1 percent argon at 0.1 millimeter of mercury pressure. The discharge conditions are: a steady direct-current plasma at 465 volts and 30 milliamperes (current-limiting resistor of 10,000 ohms included). Length L of solenoid is 5 inches (approximately 2 guide wavelengths).

* Reprinted from *Physical Review*, v. 82, p. 1255; September 15, 1951. This work was sponsored by the Signal Corps.

¹ L. Goldstein, M. A. Lampert, and J. F. Heney, "Magneto-Optics of an Electron Gas with Guided Microwaves," *Physical Review*, v. 82, pp. 956-957; June 15, 1951; also *Electrical Communication*, v. 28, pp. 233-234; September, 1951.

² S. Benner, *Naturwissenschaften*, v. 17, p. 129; 1929; H. Gutton, *Annales de Physique*, v. 13, p. 62; 1930; L. Tonks, *Physical Review*, v. 37, p. 1458; 1931; E. Appleton and F. Chapman, *Proceedings of the Physical Society*, Part 3, v. 44, pp. 246-254; May 1, 1932.

Contributors to This Issue



NATHANIEL L. COHEN

NATHANIEL L. COHEN was born on December 12, 1922, at New York City. He received the B.S. degree in electrical engineering from the College of the City of New York in 1943 and the M.S. degree from Polytechnic Institute of Brooklyn in 1949. He served as an instructor in the latter school during 1942.

From 1943 to 1948, he was with Federal Telecommunication Laboratories, where he worked on radar components and systems and on gas discharge tubes. On leave of absence, he served on a special task force for the Secretary of War during 1944 and 1945.

In 1948, he became chief engineer of Facsimile and Electronics Corporation.

• • •



J. L. GOODWIN

LADISLAS GOLDSTEIN. A photograph and biography of Dr. Goldstein appears on pages 237-238 of the September, 1951, issue.

• • •

J. L. GOODWIN was born at Chigwell, England, in 1920. He studied electrical engineering at the Borough Polytechnic and Twickenham Technical College, receiving the higher national certificate in 1947.

During the war, he did research work on underwater acoustics with the Admiralty and in 1948 he joined the staff of the transmission division of Standard Telephones and Cables.

Mr. Goodwin is a Graduate Member of the Institution of Electrical Engineers.

• • •

JOHN F. HENEY. A photograph and biography of Mr. Heney appears on page 238 of the September, 1951, issue.

• • •

G. KING received the B.Sc.Eng. degree from the City and Guilds of London College in 1938. During the following year he served that institution as a demonstrator.

From 1939 to 1945, he was at the Admiralty Signal Establishment at Witley. He then returned to his alma mater as a lecturer in communications for a year.

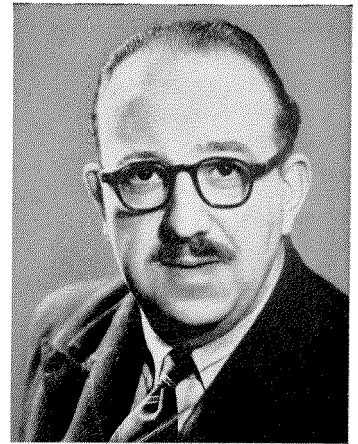
Mr. King joined Standard Telecommunication Laboratories in 1946 as head of the microwave department and is now head of the materials division. (Mr. King's paper appeared in the preceding number of this volume.)

• • •

MURRAY A. LAMPERT. A photograph and biography of Mr. Lampert appears on page 238 of the September, 1951, issue.

• • •

ERNEST G. ROWE was born in 1909 at Plymouth, England. He received from London University an honours degree in engineering in 1932 and a M.Sc. degree a year later.



ERNEST G. ROWE

He joined the development staff of the M. O. Valve Company in 1933, becoming later chief of valve development.

At the end of 1948, he was named chief receiving-valve engineer of the Brimar Valve Division of Standard Telephones and Cables, Limited.

Mr. Rowe is a Member of the Institution of Electrical Engineers, an Associate of the City and Guilds of London Institute, and holds the diploma of the Imperial College of Science and Technology.

• • •

FRIEDRICH P. SPITZER was born at Magdeburg, Germany, on June 24, 1914. He was educated in physics and applied electricity at the universities of



FRIEDRICH P. SPITZER

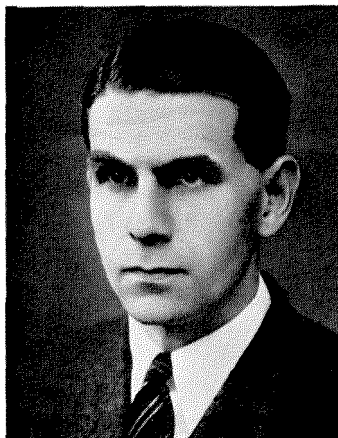
Berlin and Göttingen. After obtaining his academical degree from the University of Göttingen in 1938, he continued there doing crystal research at the Physics Institute.

From 1939 until 1945, he worked on radar developments for the German navy and then joined the staff of the Institute of Physical Chemistry at Göttingen for research on the ferroelectricity of crystals.

Since 1949, he has been engaged in the development of piezoelectric crystals at the Nuremburg laboratory of Standard Elektrizitäts-Gesellschaft A.G.

. . .

G. M. B. WILLS was born at Marlow, England, in 1915. He received the B.Sc. (Eng) degree and the A.C.G.I.



G. M. B. WILLS

from the City and Guilds (Engineering) College of the University of London.

From 1937 to 1939, he served as a development engineer for Standard Telephones and Cables, Limited. During the following seven years, he was an officer, attaining the rank of Major, in the Royal Corps of Signals. From 1942 to 1945, he was attached to the Indian Posts and Telegraphs Department and worked in that country on a telecommunication development plan.

After six months during 1946 with Standard Telephones and Cables, Limited, he joined the Brazilian Telephone Company. Recently, he was transferred from the transmission to the equipment department.

Mr. Wills is an Associate Member of the Institution of Electrical Engineers.

INTERNATIONAL TELEPHONE AND TELEGRAPH CORPORATION

Associate Manufacturing and Sales Companies

United States of America

International Standard Electric Corporation, New York, New York
Federal Telephone and Radio Corporation, Clifton, New Jersey
International Standard Trading Corporation, New York, New York
Capehart-Farnsworth Corporation, Fort Wayne, Indiana
The Coolerator Company, Duluth, Minnesota
Flora Cabinet Company, Inc., Flora, Indiana
Thomasville Furniture Corporation, Thomasville, North Carolina

Great Britain and Dominions

Standard Telephones and Cables, Limited, London, England
Creed and Company, Limited, Croydon, England
International Marine Radio Company Limited, Croydon, England
Kolster-Brandes Limited, Sidcup, England
Standard Telephones and Cables Pty. Limited, Sydney, Australia
Silovac Electrical Products Pty. Limited, Sydney, Australia
Austral Standard Cables Pty. Limited, Melbourne, Australia
New Zealand Electric Totalisators Limited, Wellington, New Zealand
Federal Electric Manufacturing Company, Ltd., Montreal, Canada

South America

Compañía Standard Electric Argentina, Sociedad Anónima, Industrial y Comercial, Buenos Aires, Argentina
Standard Electrica, S.A., Rio de Janeiro, Brazil
Compañía Standard Electric, S.A.C., Santiago, Chile

Europe

Vereinigte Telephon- und Telegraphenfabriks Aktiengesellschaft Czeija, Nissi & Co., Vienna, Austria
Bell Telephone Manufacturing Company, Antwerp, Belgium
Standard Electric Aktieselskab, Copenhagen, Denmark
Compagnie Générale de Constructions Téléphoniques, Paris, France
Le Matériel Téléphonique, Paris, France
Les Téléimprimeurs, Paris, France
C. Lorenz, A.G. and Subsidiaries, Stuttgart, Germany
Mix & Genest Aktiengesellschaft and Subsidiaries, Stuttgart, Germany
Süddeutsche Apparatefabrik Gesellschaft m.b.H., Nuremberg, Germany
Nederlandsche Standard Electric Maatschappij N.V., The Hague, Netherlands
Fabbrica Apparecchiature per Comunicazioni Elettriche, Milan, Italy
Standard Telefon og Kabelfabrik A/S, Oslo, Norway
Standard Electrica, S.A.R.L., Lisbon, Portugal
Compañía Radio Aérea Marítima Española, Madrid, Spain
Standard Eléctrica, S.A., Madrid, Spain
Aktiebolaget Standard Radiofabrik, Stockholm, Sweden
Standard Telephone et Radio S.A., Zurich, Switzerland

Telephone Operating Systems

Compañía Telefónica Argentina, Buenos Aires, Argentina
Compañía Telefónico-Telefónica Comercial, Buenos Aires, Argentina
Compañía Telefónico-Telefónica del Plata, Buenos Aires, Argentina
Companhia Telefônica Nacional, Porto Alegre, Brazil
Compañía de Teléfonos de Chile, Santiago, Chile
Compañía Telefónica de Magallanes S.A., Punta Arenas, Chile
Cuban American Telephone and Telegraph Company, Havana, Cuba
Cuban Telephone Company, Havana, Cuba
Compañía Peruana de Teléfonos Limitada, Lima, Peru
Porto Rico Telephone Company, San Juan, Puerto Rico

Radiotelephone and Radiotelegraph Operating Companies

Compañía Internacional de Radio, Buenos Aires, Argentina
Compañía Internacional de Radio Boliviana, La Paz, Bolivia
Companhia Radio Internacional do Brasil, Rio de Janeiro, Brazil
Compañía Internacional de Radio, S.A., Santiago, Chile
Radio Corporation of Cuba, Havana, Cuba
Radio Corporation of Porto Rico, San Juan, Puerto Rico

Cable and Radiotelegraph Operating Companies

(Controlled by American Cable & Radio Corporation, New York, New York)

The Commercial Cable Company, New York, New York¹
Mackay Radio and Telegraph Company, New York, New York²
All America Cables and Radio, Inc., New York, New York³
Sociedad Anónima Radio Argentina, Buenos Aires, Argentina⁴

¹Cable service. ²International and marine radiotelegraph services.
³Cable and radiotelegraph services. ⁴Radiotelegraph service.

Laboratories

Federal Telecommunication Laboratories, Inc., Nutley, New Jersey
International Telecommunication Laboratories, Inc., New York, New York
Laboratoire Central de Télécommunications, Paris, France
Standard Telecommunication Laboratories, Limited, London, England